MANIPULATING AND EXTENDING THE COHERENCE OF HOLE SPINS

JOSÉ CARLOS ABADILLO-URIEL

CEA GRENOBLE

OUTLINE

1) Introduction.
2) Manipulation of hole qubits
3) Coherence
4) Spin-photon coupling
5) Conclusions

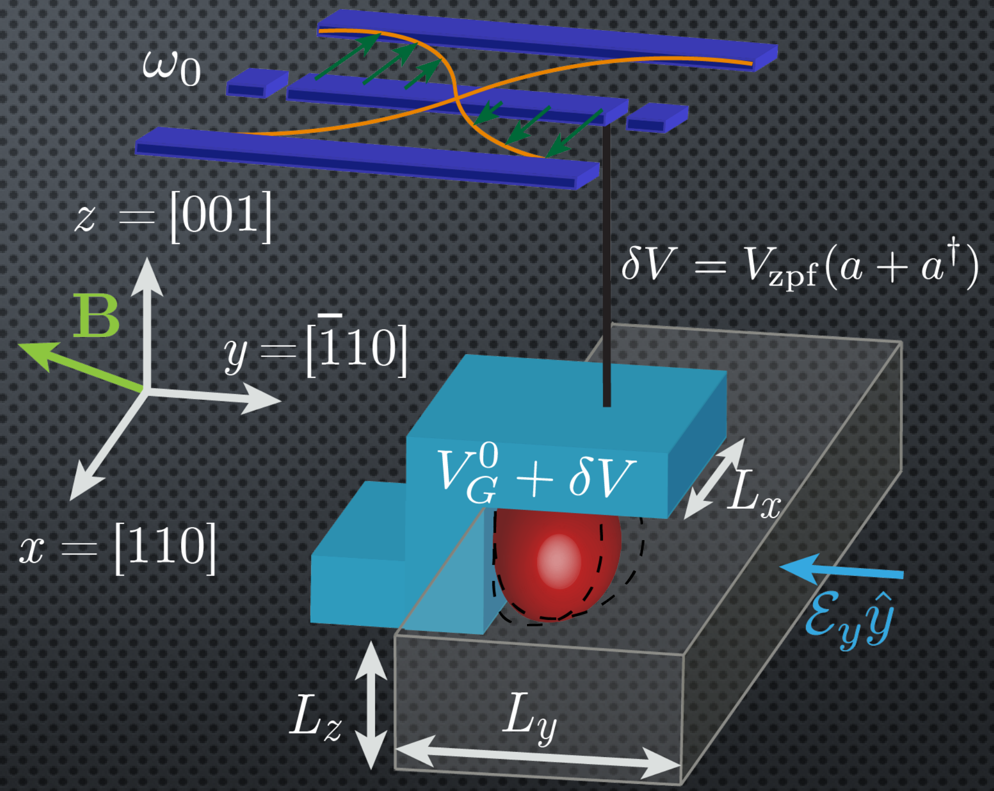

1. Introduction

- Why build a QC? Efficciency
  - Information security. Shor algorithm for prime factorization. Quantum cryptography.
  - Database search. Grover algorithm.
  - Quantum simulations.
  - For the fun of it

INTRODUCTION

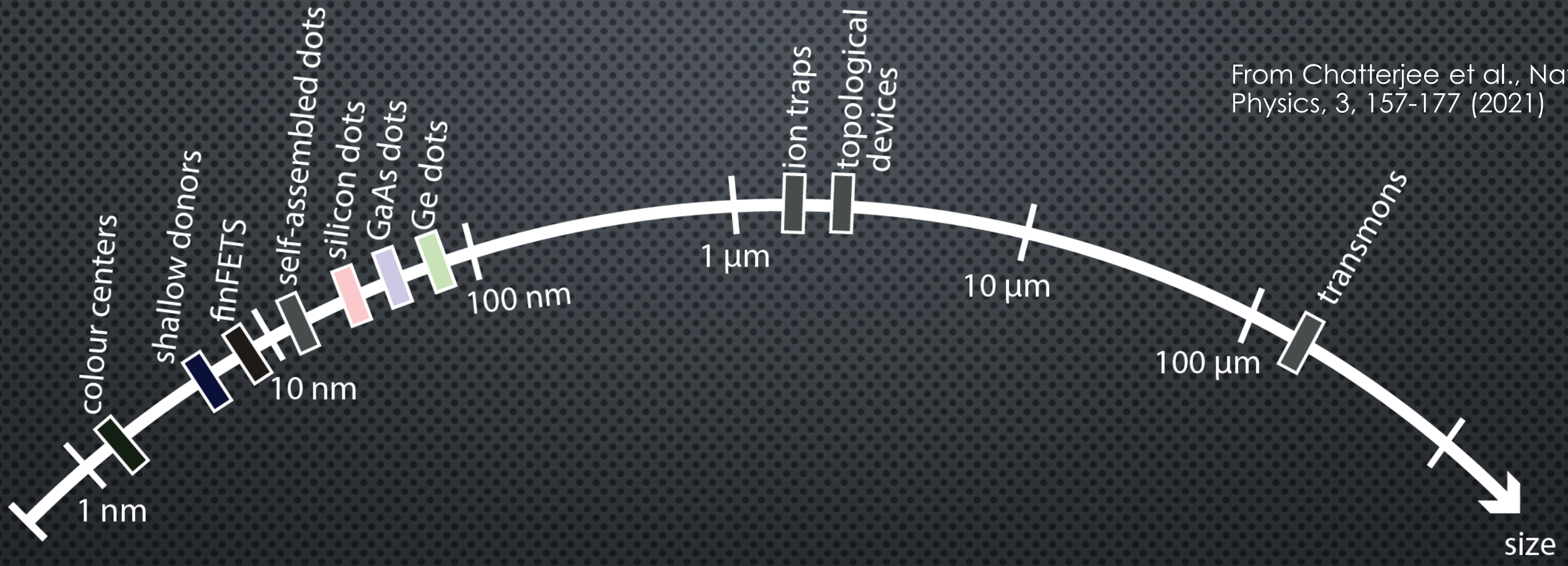

From Chatterjee et al., Nature Reviews Physics, 3, 157-177 (2021)

Transmons are leading the race

Si and Ge QDs are particularly promising for quantum computing purposes

MOTIVATION

From Chatterjee et al., Nature Reviews Physics, 3, 157-177 (2021)

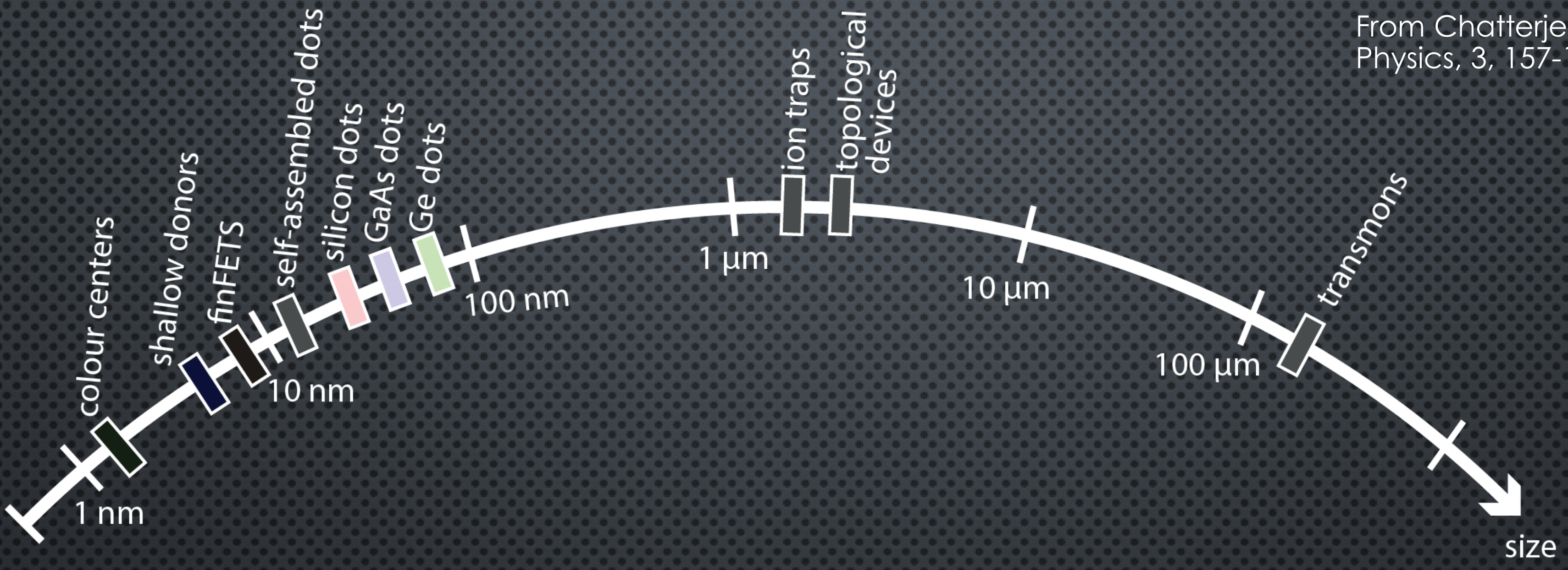

Industrially compatible

Good coherence times & gate manipulability

Prospects of scalability (small unit cell)

High-temperature operation (4K)

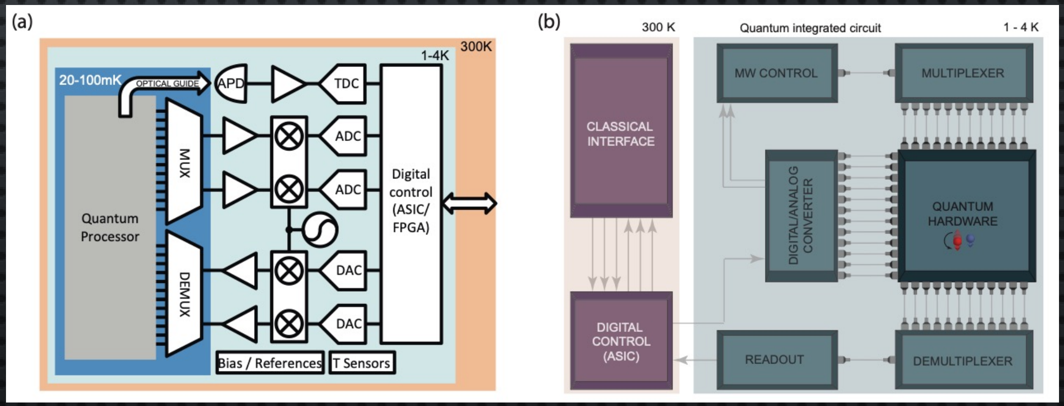

From Petit et al., Nature 580, 355-359 (2020)

BASIC OPERATION OF QD QUBITS

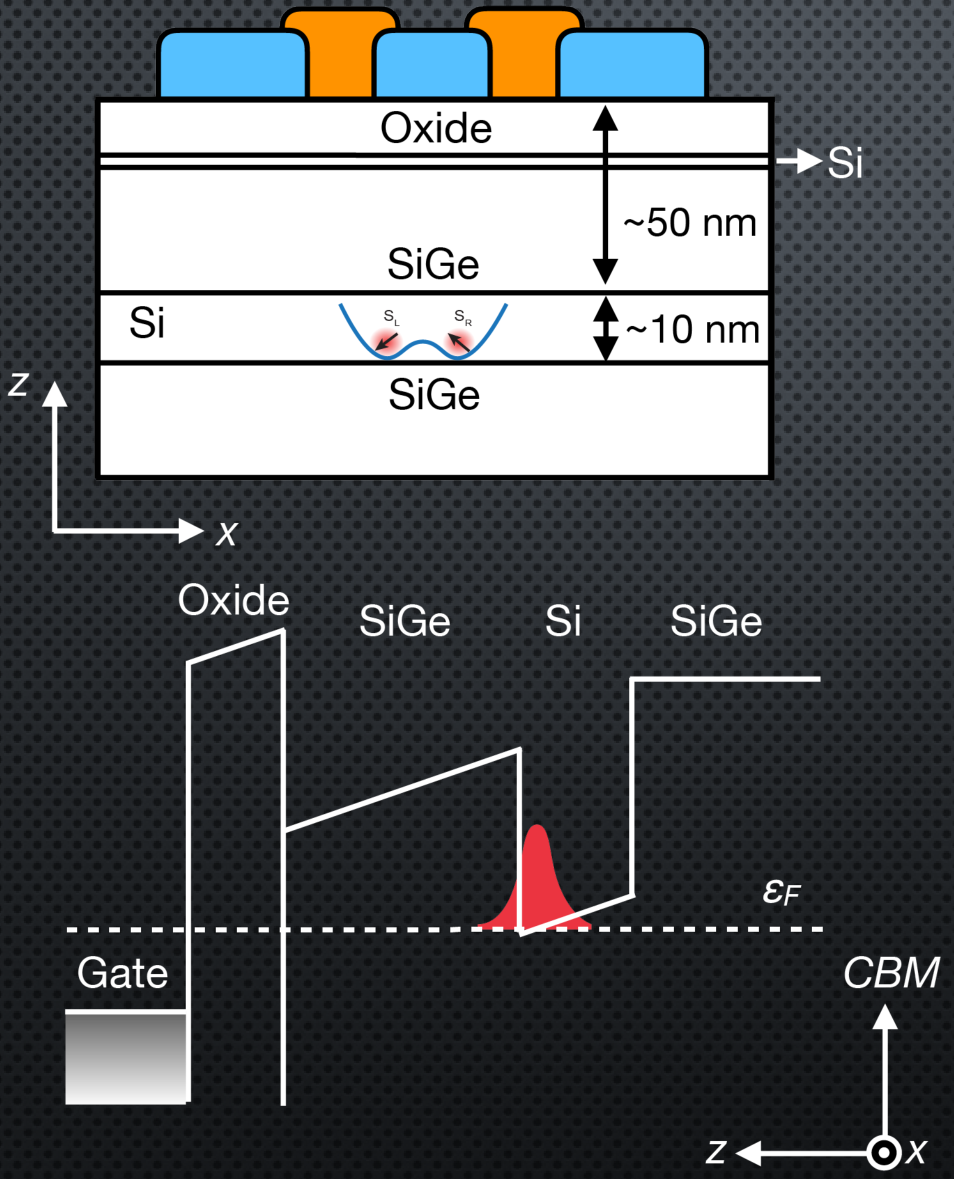

- Electrons/holes are confined in a quantum well
- The electron/hole is pushed against the interface
- Gates are used to manipulate the qubits
- Readout: spin-to-charge conversión
- Original implementations in GaAs/AlGaAs heterostructures

STATUS

-High single-qubit gate fidelities have been demonstrated. See

Nature Nanotechnology **13**, 102-106 (2018)

Nature volume **569**, pages 532–536 (2019)

Nature Communications volume 11, Article number: 4144 (2020)

-Two-qubit gates beyond QEC threshold. See

Nature **601**, 343-347 (2022)

-Working six-qubit processor with electrons

Nature ***609****, 919–924 (2022)*

Nature **591**, 580–585 (2021)

-4K operation demonstrated

Nature 580, 355-359 (2020)

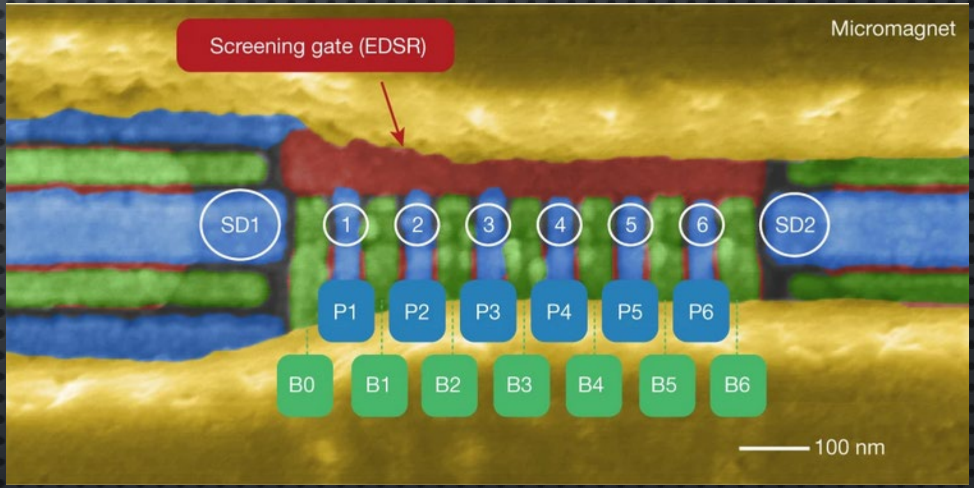

HOLE SPIN-ORBIT QUBITS

Hole spins in Si/Ge inherit the spin-orbit interaction from the valence band

Spin degree of freedom is coupled to the movement of the hole: allows all-electrical manipulation of the hole

Qubit properties are highly tunable through gate voltages

Cool physics: anisotropic g-matrices, Rashba SOC, sweet spots

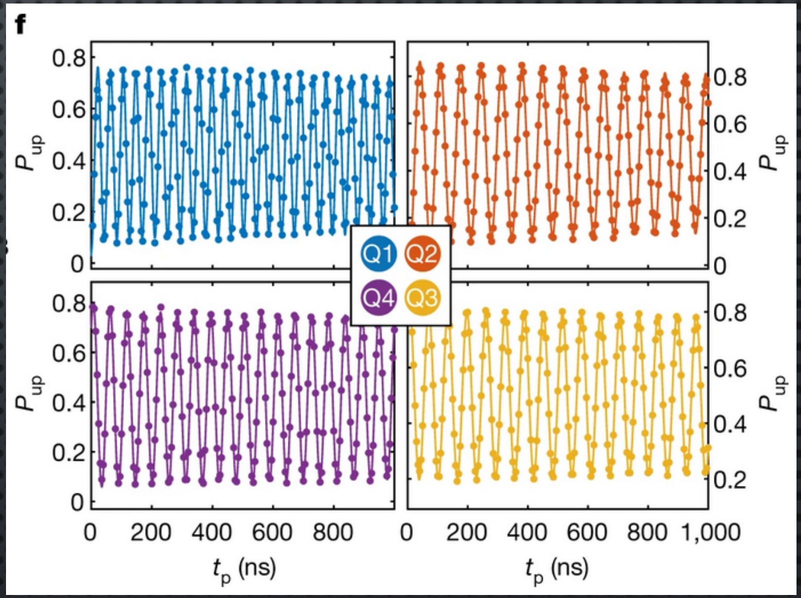

Hendrickx et al., Nature 591, 580–585 (2021)

QUICK GROWTH

- Demonstrations of hole qubit in Si and Ge
  Maurand et al., Nat. Comms. 7, 13575 (2016)
  Hendrickx et al., Nat. Comms. 11, 3478 (2020)

- 4-qubit processor: single-qubit gates above 99.9% and two-qubit above 99%
  Hendrickx et al., Nature 577, 487–491 (2020)
  Hendrickx et al., Nature 591, 580–585 (2021)

- Large coherence T_2^*~90 μs
  Piot et al., Nat. Nano (2022)

- "Hot"-qubit operation ~ 4K
  Carmenzind et al., Nat. Electronics 5, 178–183 (2022)

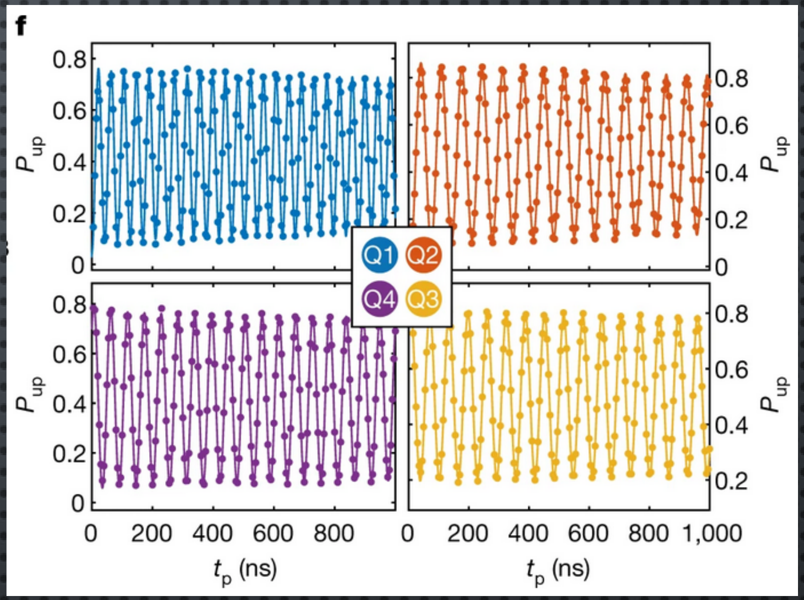

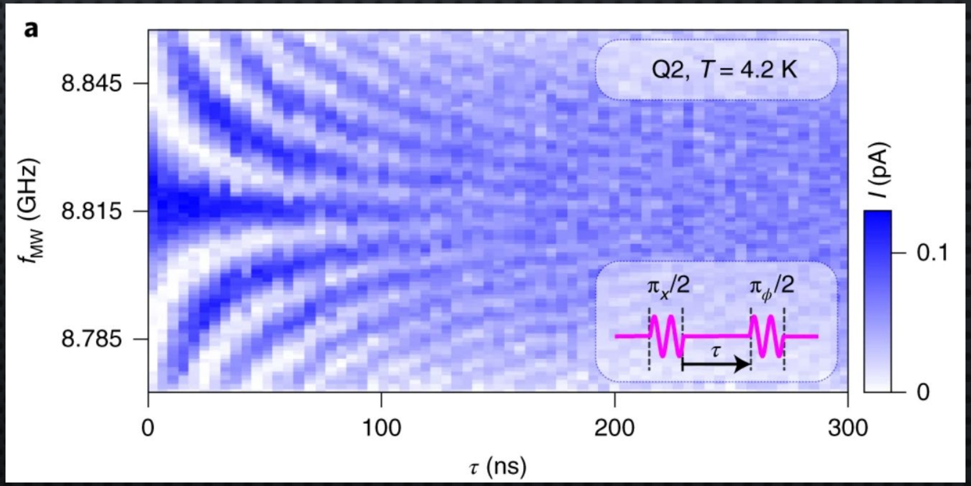

2. HOLE SPIN MANIPULATION

-Hole spin is coupled to its motion

-Rashba SOC

-gTMR = modulate the g-tensor by changing the hole shape

$$H_Q = \frac{\mu_B}{2}\boldsymbol{B}\cdot g_h\boldsymbol{\sigma} + \left(\frac{em}{\hbar}\frac{l^4}{l_{so}}\boldsymbol{b_{so}}\cdot\boldsymbol{\sigma}\right)\partial_t E_{ac}^z(t) + \left(\frac{\mu_B}{2}\boldsymbol{B}\cdot\partial_E g_h\boldsymbol{\sigma}\right)E_{ac}^{\perp}(t)$$

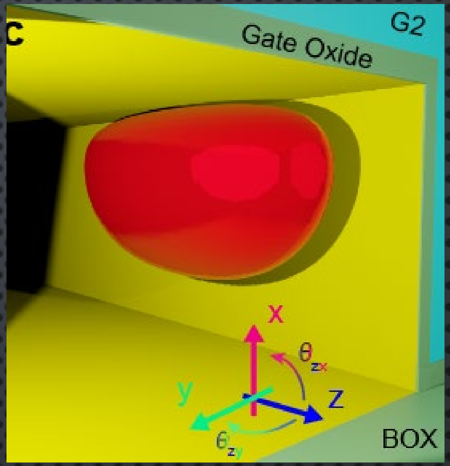

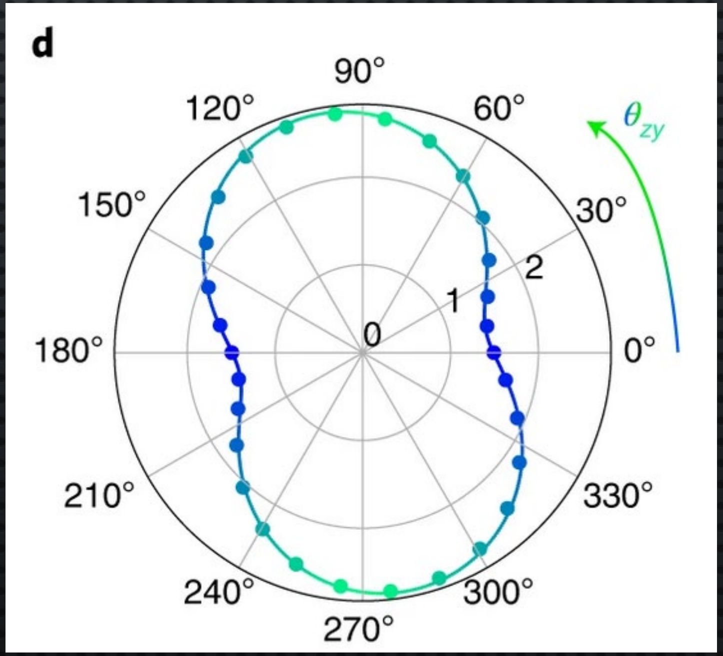

RASHBA SOC

-Lack of inversion symmetry. Determined by geometry and gates

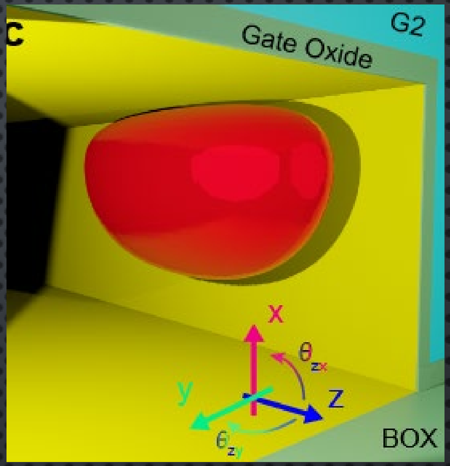

-Planar isotropic dots (cubic Rashba)

$$p_\pm = p_x \pm i p_y$$

$$\gamma_\pm = (\gamma_3 \pm \gamma_2)/2$$

$$H_{SO} = \alpha_1 p_-^3 \sigma_+ + \alpha_2 p_+ p_- p_+ \sigma_+ + h.c.$$

$$\alpha_1 \propto \gamma_+ \langle \mathrm{HH}|p_z|\mathrm{LH}\rangle \quad \alpha_2 \propto \gamma_- \langle \mathrm{HH}|p_z|\mathrm{LH}\rangle$$

-Nanowire or anisotropic dots (linear Rashba). See Golovach et al. (2006) PRB 74

$$H_{SO} = \frac{\hbar}{m l_{so}} p_x \sigma_y$$

$$\frac{1}{l_{so}} \propto \gamma_+ \langle \mathrm{HH}|p_-|\mathrm{LH}\rangle$$

Michal et al., Phys. Rev. B 103, 045305 (2021)
Bosco et al., Phys. Rev. B 104, 115425 (2021)

G-TMR

-g-factor is anisotropic. By driving g-tensor the hole feels a time-dependent magnetic field

-Pure heavy-hole have large vertical g-factors vs weak in-plane g-factors

-Pure light-holes have large in-plane g-factors and weak vertical g-factors

-HH-LH admixture is gate tunable

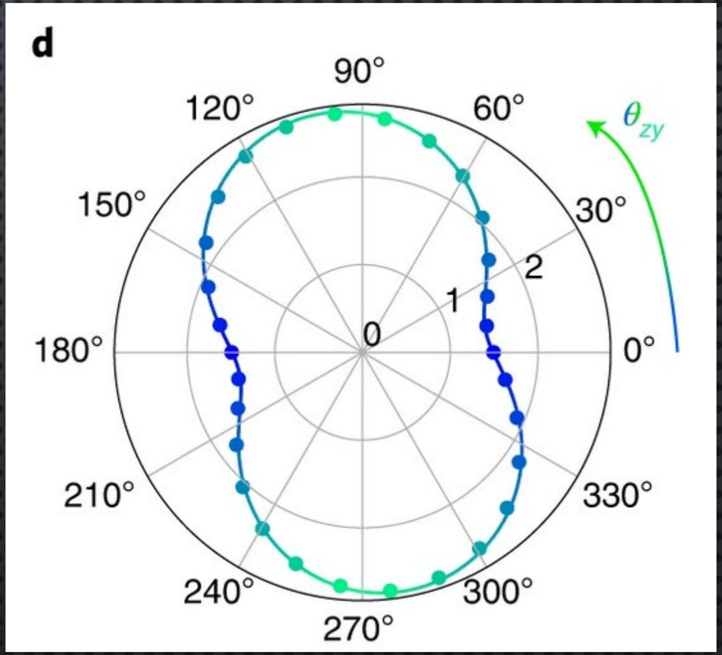

$$f_R = \frac{\mu_B B V_{ac}}{2hg^*} |(g \cdot b) \times (g' \cdot b)|$$

Crippa *et al.* (2018) *PRL* **120**
Kato *et al.* (2003) *Science* **229**

SOME MECHANISMS MAY STILL BE MISSING

-The experiments in Delft use in-plane magnetic field with planar Ge: cubic Rashba

$$H_{SO} = \alpha_1 p_-^3 \sigma_+ + \alpha_2 p_+ p_- p_+ \sigma_+ + h.c.$$

-g-tmr in planar dots with in-plane field is also inefficient

$$f_R = \frac{\mu_B B V_{ac}}{2hg^*} |(g \cdot b) \times (g' \cdot b)|$$

In total:

$$H_Q = \frac{\mu_B}{2} \boldsymbol{B} g_x \boldsymbol{\sigma_x} + H_{SO} + \frac{\mu_B}{2} \boldsymbol{B} \delta g_x(t) \boldsymbol{\sigma_x}$$

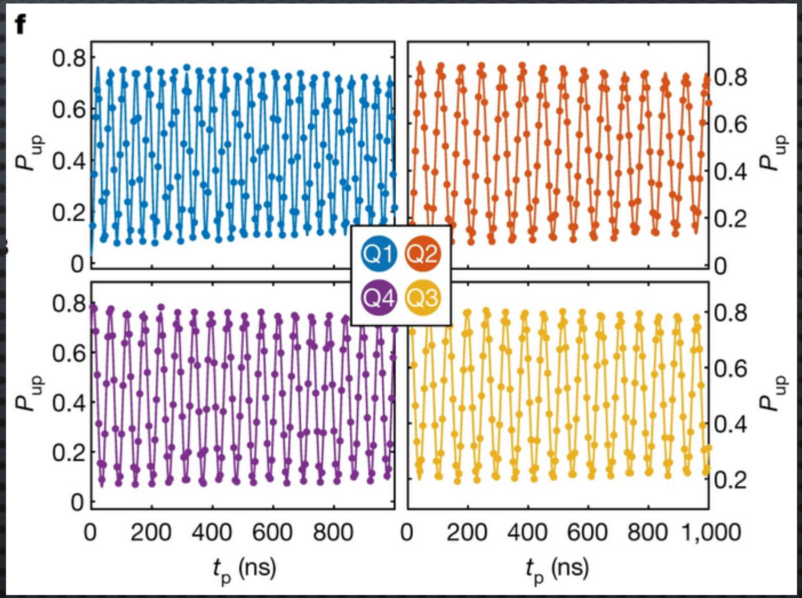

REALISTIC SIMULATIONS

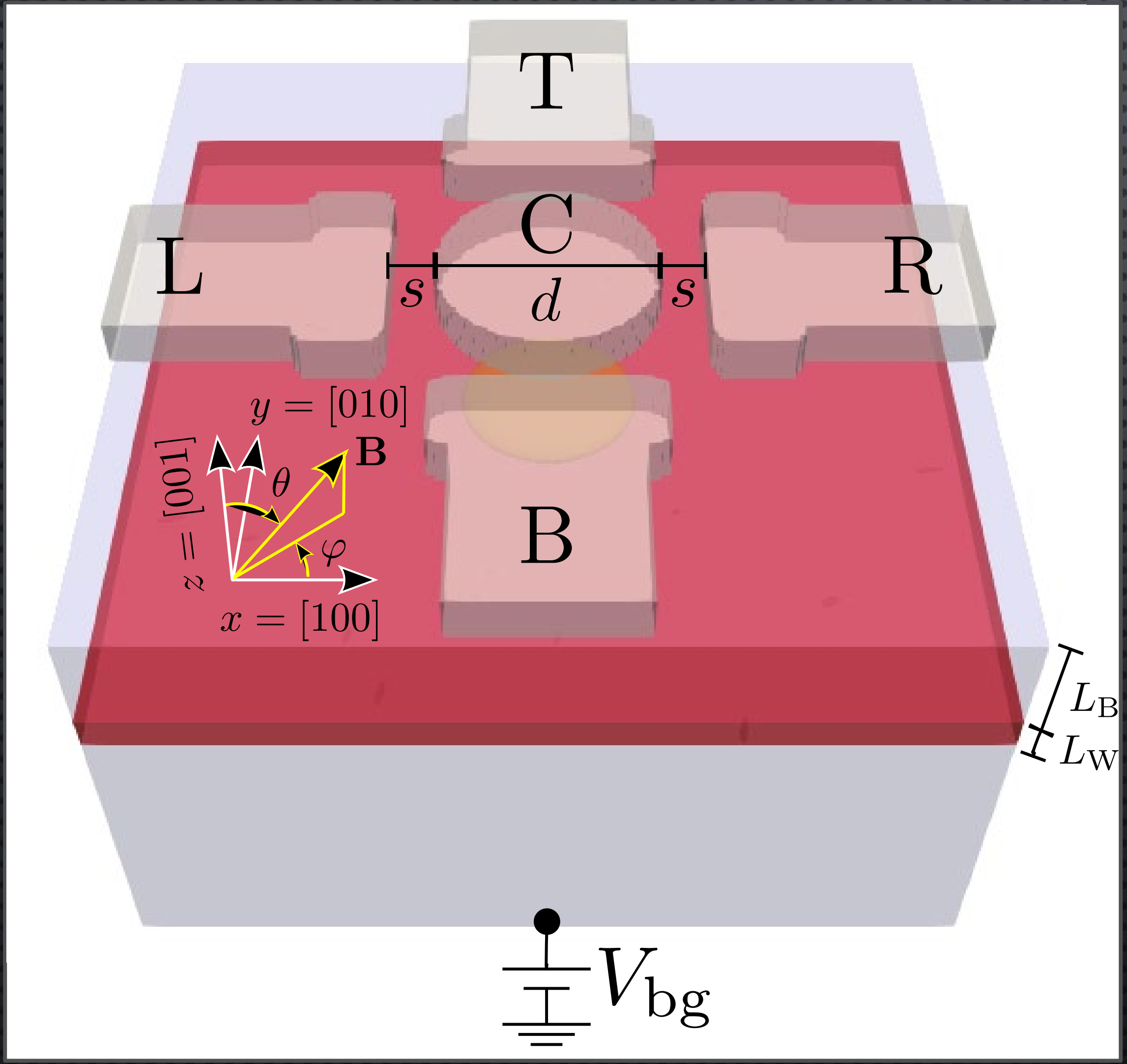

$$f_R = \frac{\mu_B B V_{ac}}{2hg^*} |(g \cdot b) \times (g' \cdot b)|$$

See arXiv:2209.10231

NUMERICAL EXPERIMENT IS CONSISTENT WITH THE OBSERVATION

-Prominent peak of Rabi frequencies when the magnetic field is aligned along the in-plane direction parallel to the drive

-Cubic Rashba should lead to a growing background in the vertical direction

-A peculiarity: at zero vertical field, the feature is maximized (opposite to Rashba)

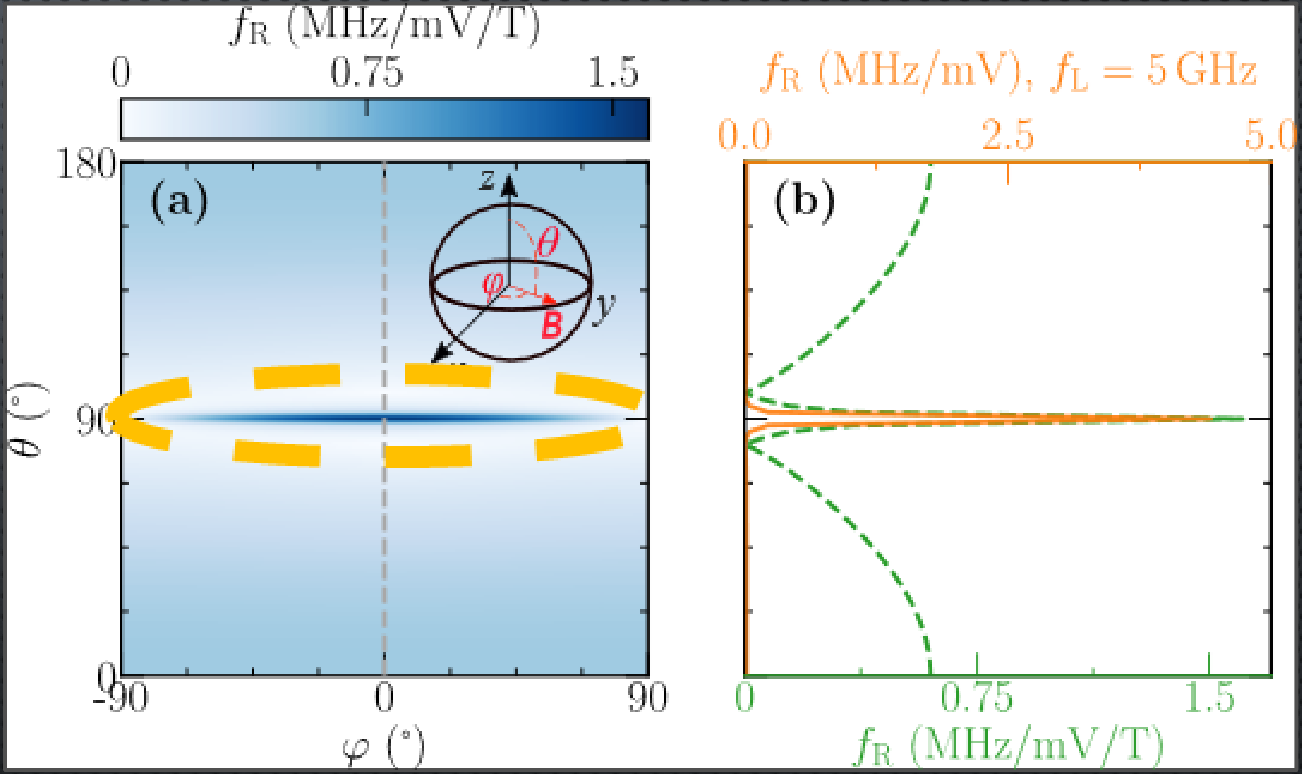

$$f_R = \frac{\mu_B B V_{ac}}{2hg^*} |(g \cdot b) \times (g' \cdot b)|$$

KEY INGREDIENT IS THE REALISTIC ELECTROSTATICS

-Potential is usually modelled as harmonic separable

$$V(x,y,z) = \frac{1}{2} m_{eff} \omega^2 (x^2 + y^2) + eF_z z$$

-We noticed that the minimal ingredient for the in-plane feature was non-separability

$$V(x,y,z) = \frac{1}{2} m_{eff} \omega^2 (x^2 + y^2) \zeta(z)^2 + eF_z z$$

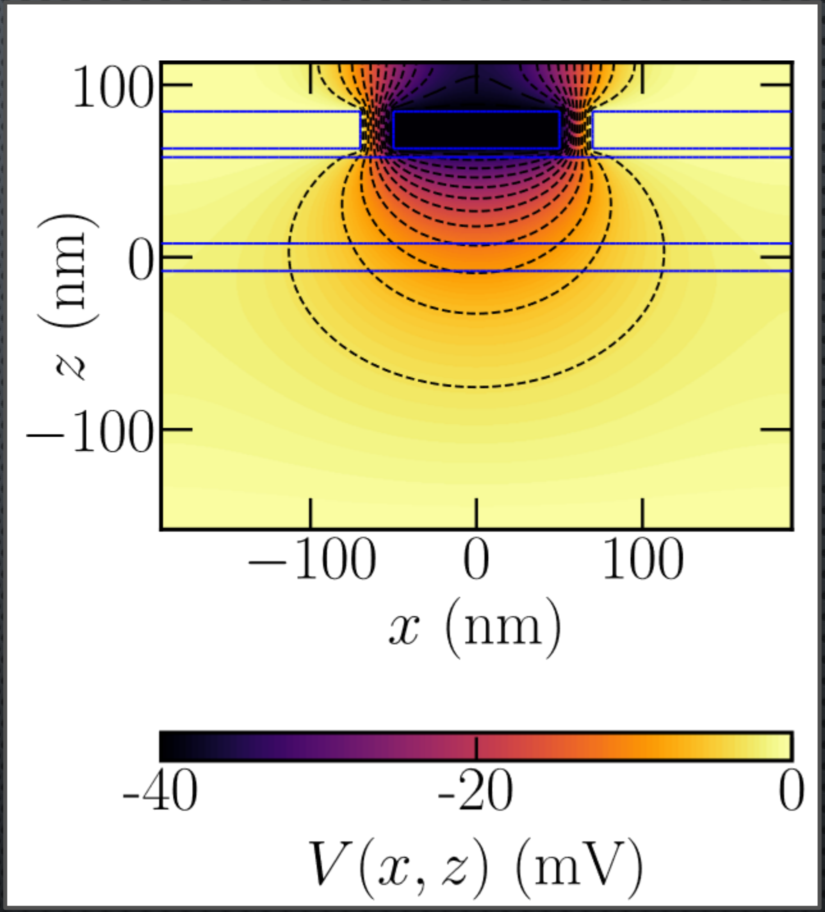

WE CAN CAPTURE THE PHYSICS WITH A NON SEPARABLE POTENTIAL

$$H_0 = \underbrace{\begin{pmatrix} P+Q & -S & R & 0 \\ -S^* & P-Q & 0 & R \\ R^* & 0 & P-Q & S \\ 0 & R^* & S^* & P+Q \end{pmatrix}}_{\text{(1)}} \overbrace{+ 2\mu_B \left(\kappa \mathbf{B}\cdot\mathbf{J} + q\mathbf{B}\cdot\mathbf{J}^3\right)}^{\text{(2)}} + \underbrace{\frac{1}{2} m_0 \omega_0^2 \left(x^2+y^2\right)}_{\text{(3)}} \overbrace{\zeta\left(z\right)^2}^{\text{(4)}} \underbrace{- \left(\nu+1\right) b_v \varepsilon_{\parallel} J_z^2}_{\text{(5)}}$$

(1): Luttinger-Kohn Hamiltonian, kinetic part

(2): Zeeman, magnetic contribution

(3): In-plane harmonic confinement

(4): Coupling in-plane and vertical motion

(5): Strain

The effective Hamiltonian for GS heavy-hole subspace can be obtained through Schrieffer-Wolff transformation. The subbands couple through

$$\mathcal{H}_{hh'} \approx \frac{1}{\Delta_{\mathrm{LH}}} \sum_l \langle 0,h| H_c |0,l\rangle \langle 0,l| H_c' |0,h'\rangle$$

$$\mathcal{H} = \frac{\mu_B}{2} \boldsymbol{\sigma} \cdot \mathbf{g}\mathbf{B} + \frac{1}{2}\mu_B \delta V(t) \left(\lambda_x B_x + \lambda_y B_y\right) \sigma_z$$

When the potential is separable $\lambda_{x,y} = 0$

Physically, it is similar to a gTMR mechanism

TAKE HOME MESSAGES

Non-separability mechanism can explain the experimental results in planar dots

Neither Rashba nor conventional gTMR explain in-plane manipulation of 2D isotropic dots

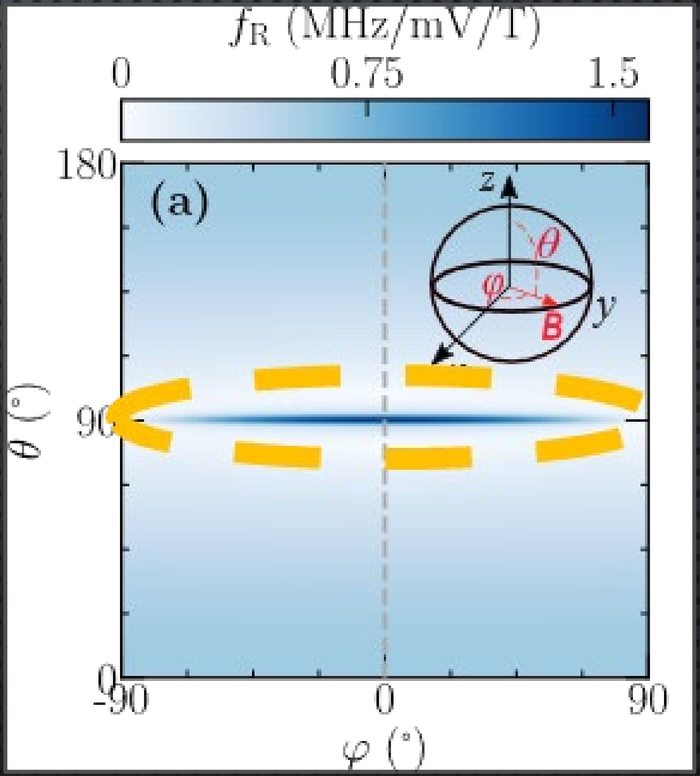

3. HOLE SPIN COHERENCE

-At the moment we couple the spin to the motion, charge noise warms up

-Charge noise is ubiquitous in these nanostructures

-Is it possible to mitigate noise at the levels of electron qubits?

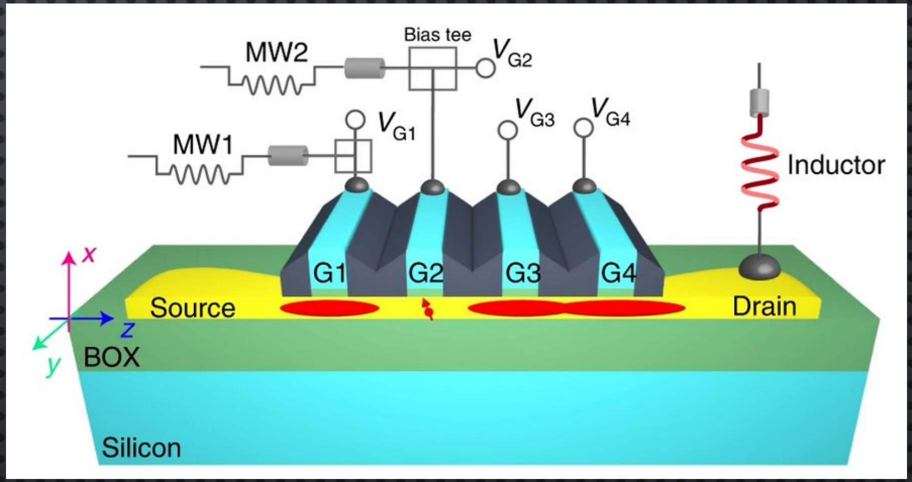

Nature Nanotechnology 17, 1072–1077 (2022)

COHERENCE EXPERIMENT

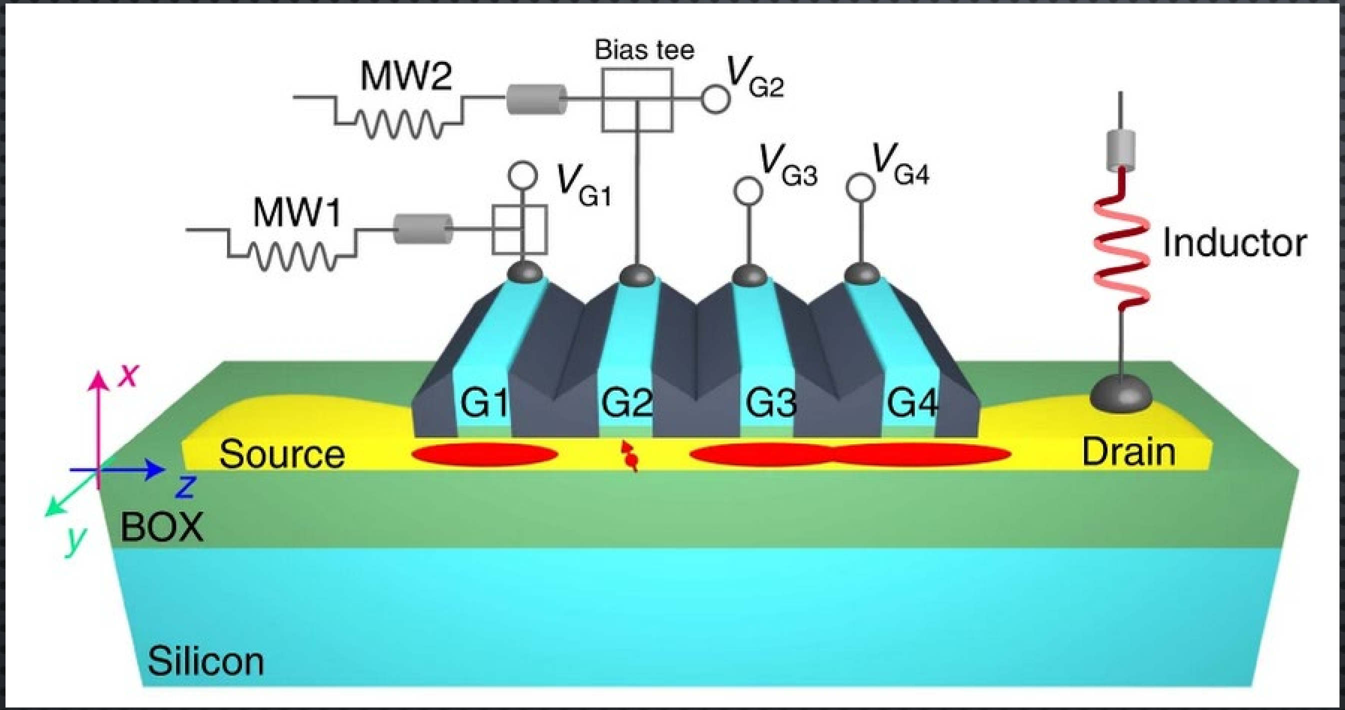

Nature Nanotechnology 17, 1072–1077 (2022)

-Natural silicon nanowire

-Spin under G2 is qubit

-Elzerman readout

MODELING THE EXPERIMENT

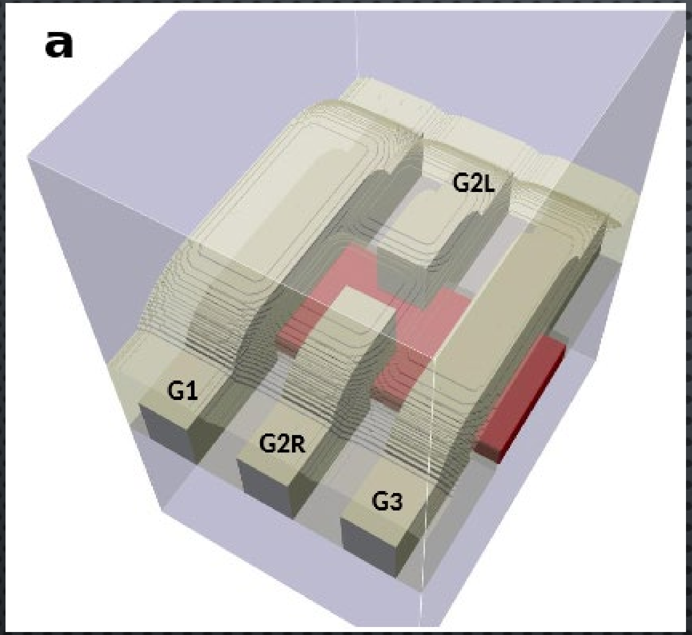

Nature Nanotechnology 17, 1072–1077 (2022)

Same process as before but with the nanowire experiment

MEASURING G-FACTORS

-The g-factor anisotropies are measured as a function of magnetic field angle

$$g = hf_L/\mu_B B$$

-Model captures very well the anisotropy (HH-LH mixing)

-Rotated g-factors coming from residual shear strain

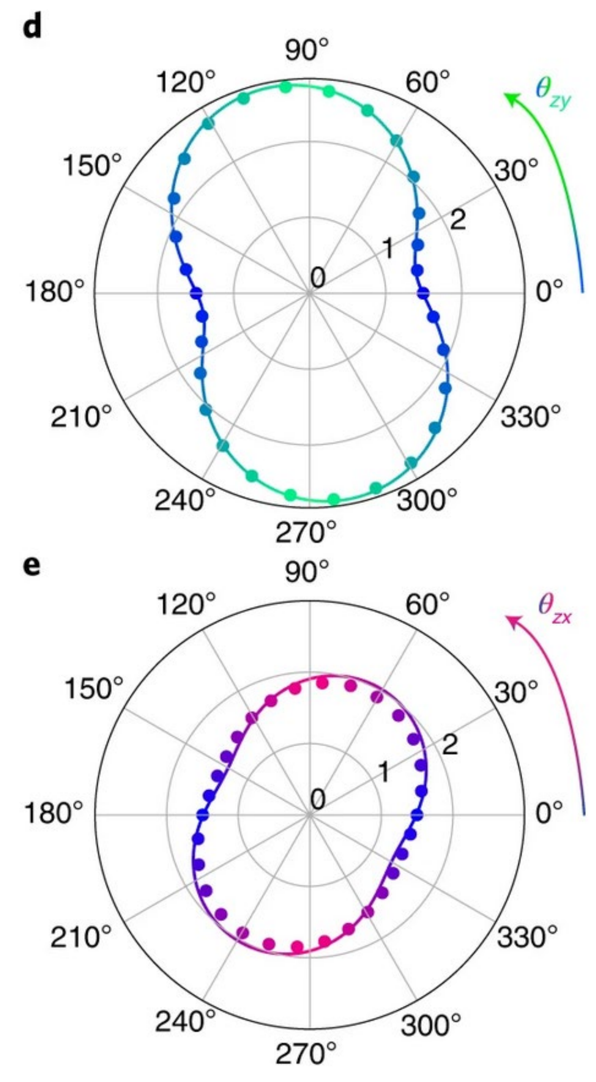

NOISE SUSCEPTIBILITY

-The Larmor frequency changes for different gate voltages and the derivative can be measured

$$g(V) = hf_L(V)/\mu_B B$$

-For G2, sweet spots appear ~40 deg and ~110 deg-

-In G1 there is no real sweet spot in this configuration

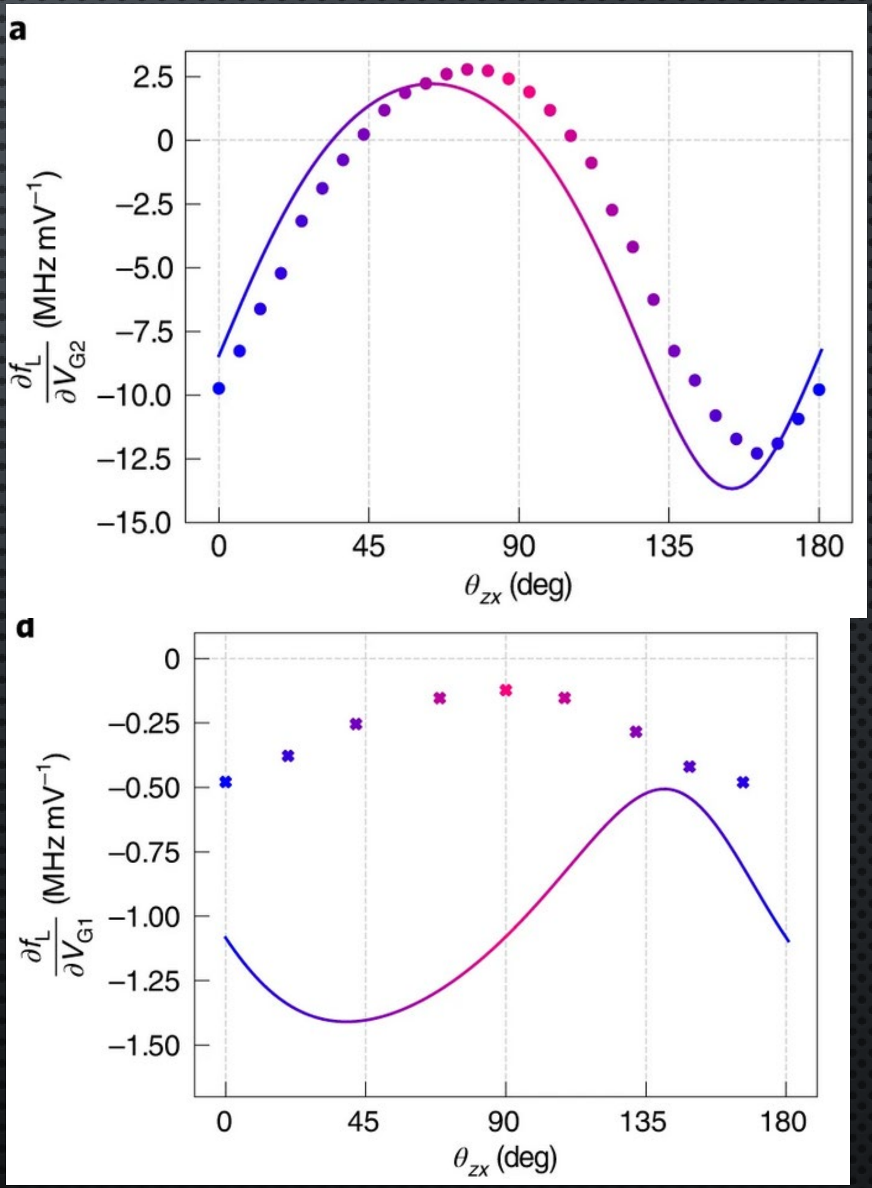

SPIN ECHO TIMES

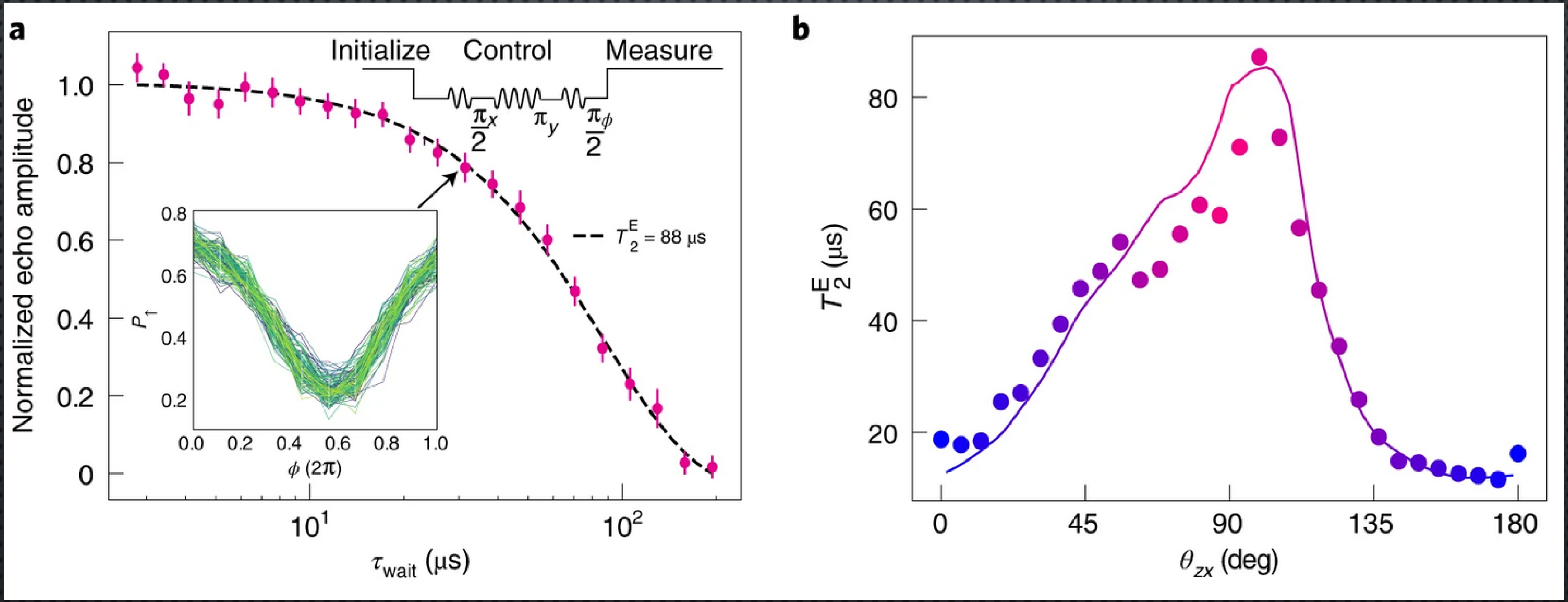

Coherence time is maximal near 90 deg near one of the G2 sweet spots and the G1 minimal susceptibility point

TAKE HOME MESSAGES

Coherence times of holes can be comparable to electrons with micromagnets

CPMG allowed to extend coherence up to 0.4 ms

Hyperfine noise limits free induction decay to ~1 microsecond

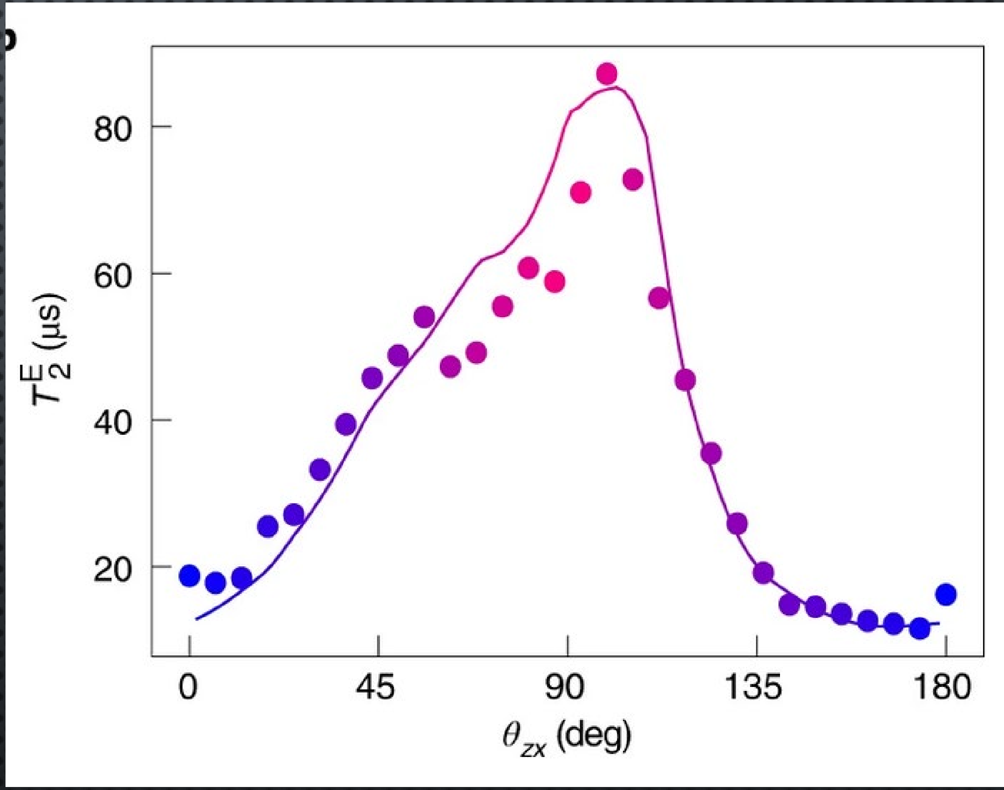

4. SPIN-PHOTON COUPLING

Interaction distance

$\sim 50nm$

$\sim 50nm - 50\mu m$

$\sim 1cm$

Nearest neighbor exchange interaction

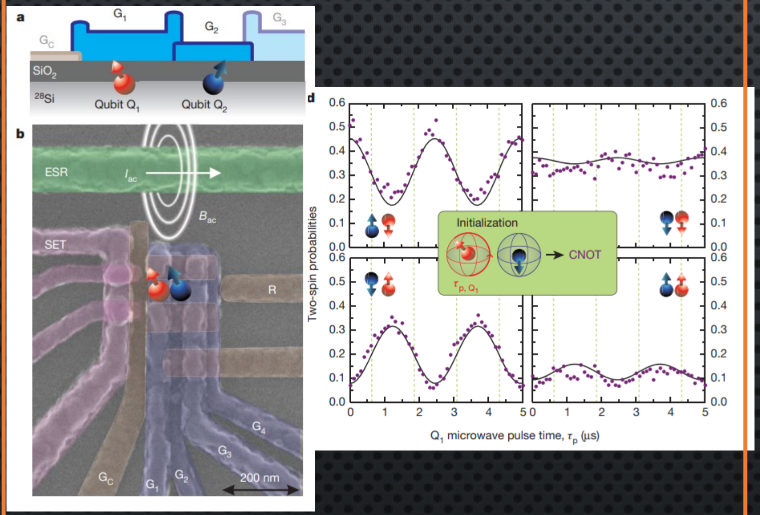

Veldhorst et al., Nature **526** (2015)

Charge shuttling in a QD array

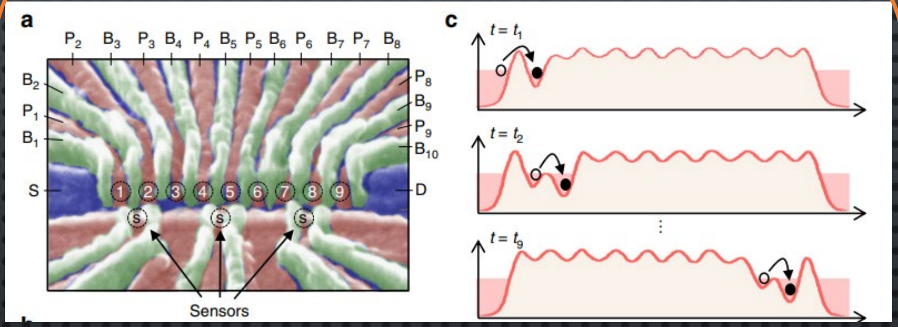

Mills et al., Nat. Comm. **10** (2019)

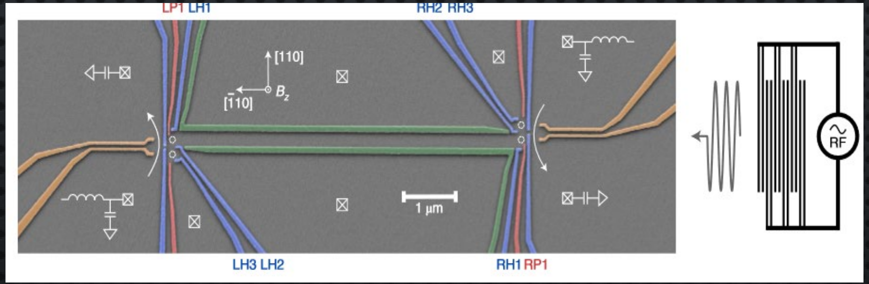

Jadot et al., Nat. Nano. 16, 570–575 (2021)

Photon mediated interaction

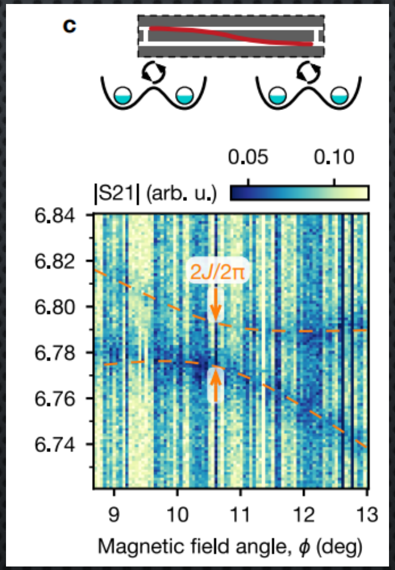

Harvey-Collard et al., PRX **12** (2022)

ELECTRON-PHOTON INTERFACES IN SI

Photons couple readily to the charge of the electron

To couple the spin to the photon one needs to induce an artificial SOC: micromagnets

Coupling in the tens MHz
Decoherence rates in few MHz

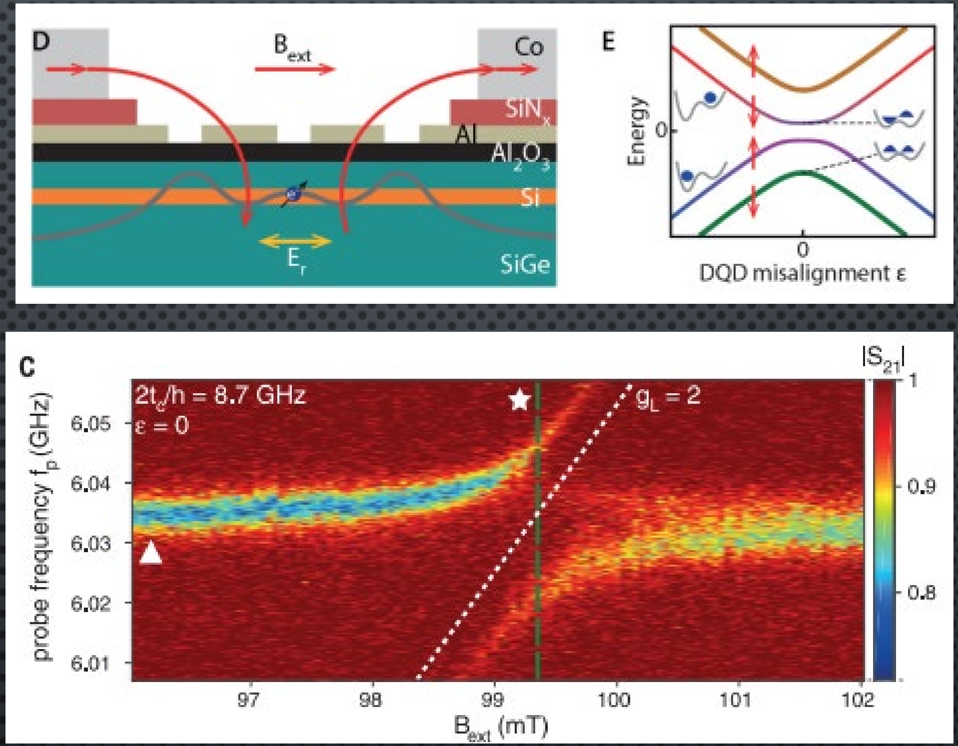

Samkharadze et al.
Science 359, 1123 (2018)

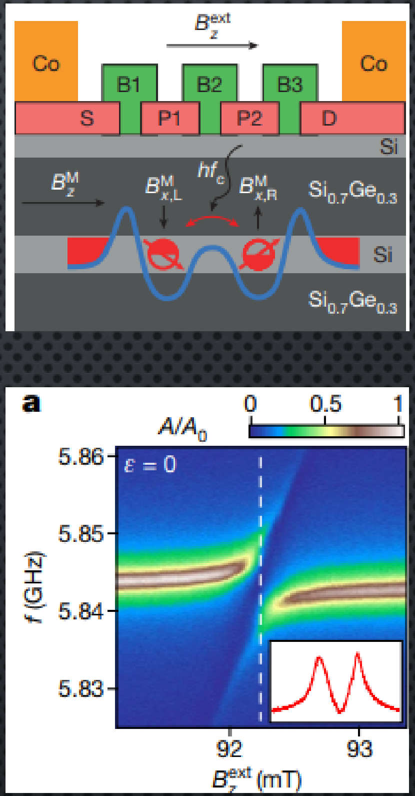

Mi et al.
Nature 555, 590 (2018)

What if we take advantage of the intrinsic SOC of holes?

arXiv:2206.14082

CIRCUIT QED WITH HOLE SPINS IN SI

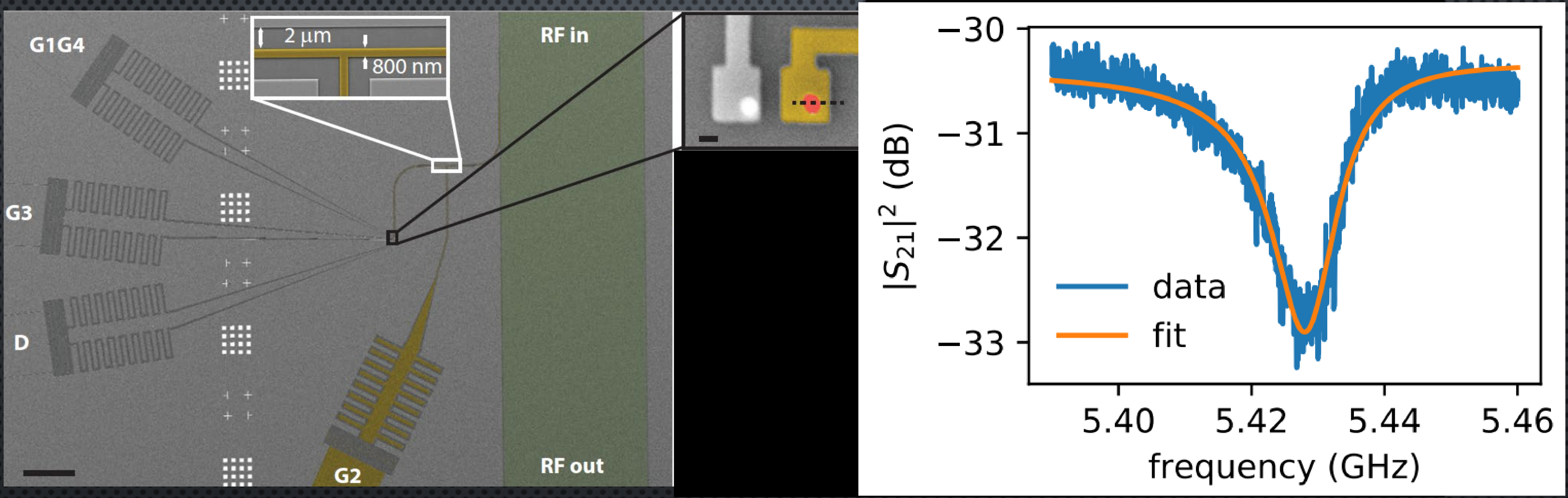

$\omega_r/2\pi = 5.43$ GHz

$\kappa/2\pi = 13.5$ MHz

$\kappa_{int}/2\pi = 10$ MHz

$\kappa_{ext}/2\pi = 3.5$ MHz

- $\lambda/2$ NbN CPW resonator $Z_c = 2\ k\Omega$, $f_r = 5.4$ GHz
- Co-fabrication with resonator at interconnect layer (M1), connected by W vias
- Si nanowire transistor on SOI with one gate connected to the resonator

CIRCUIT QED WITH HOLE SPINS IN SI

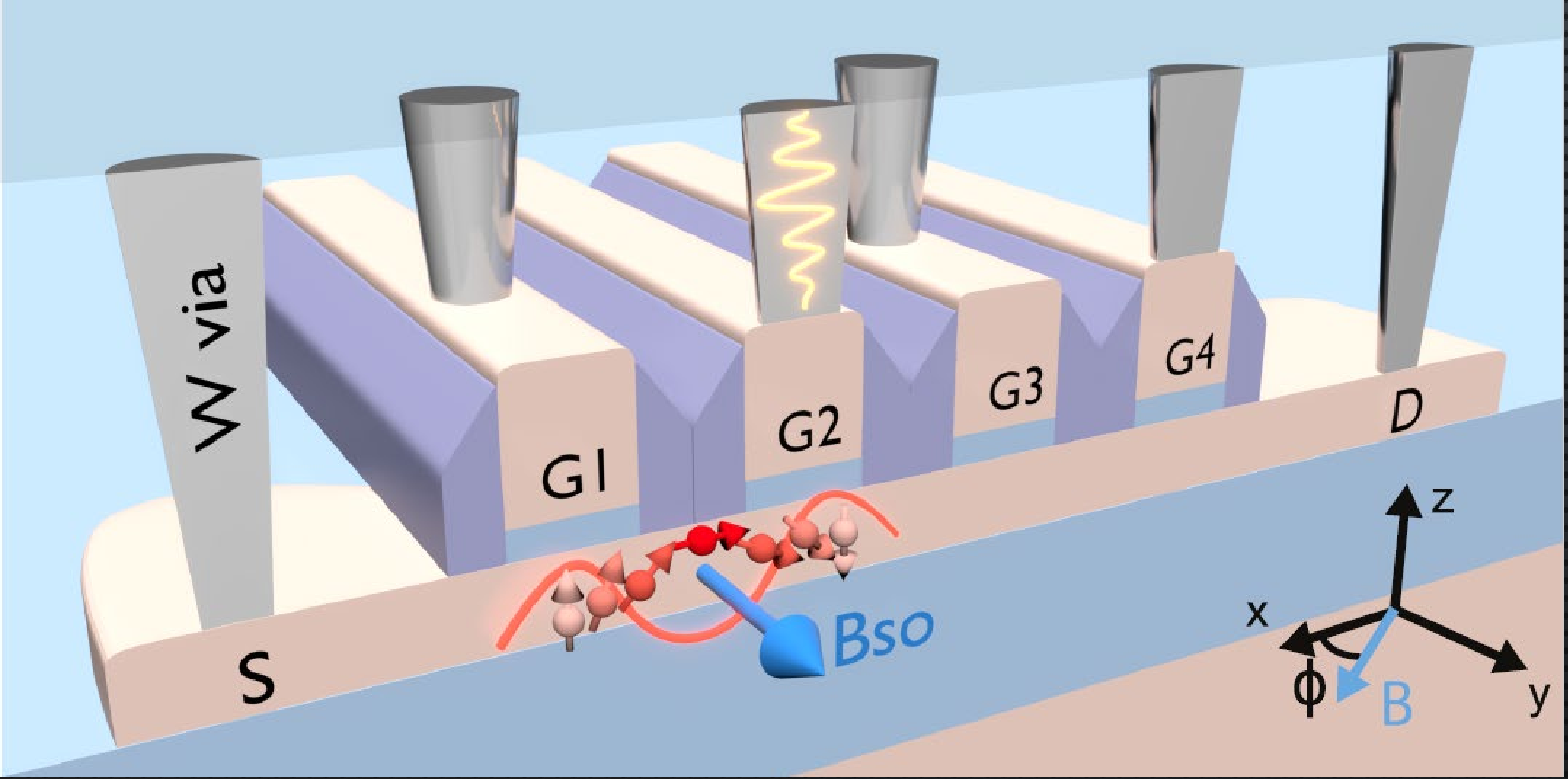

CHARGE-PHOTON INTERACTION

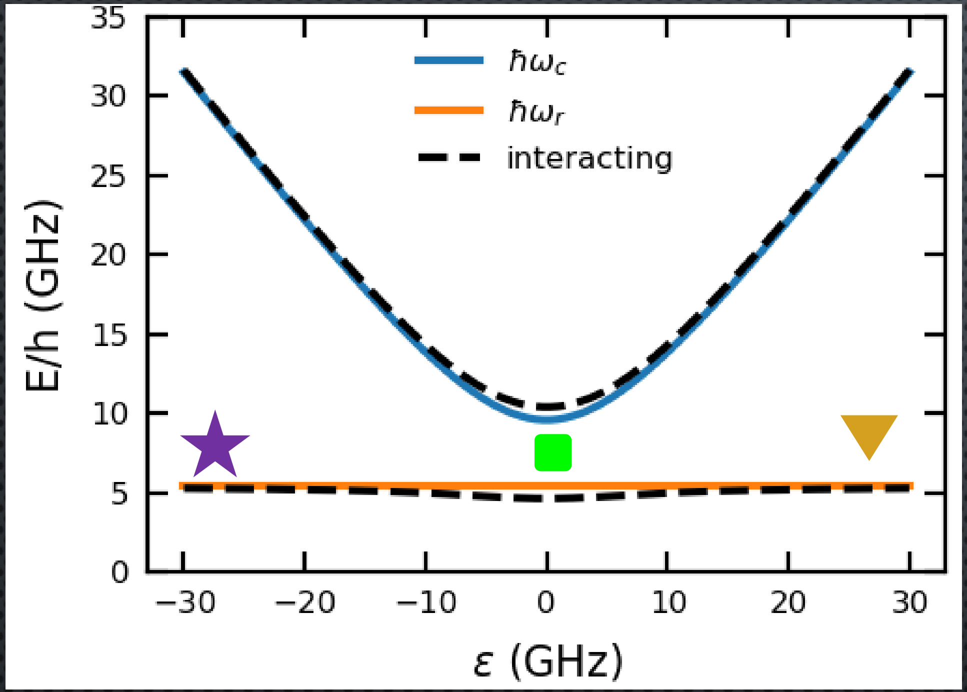

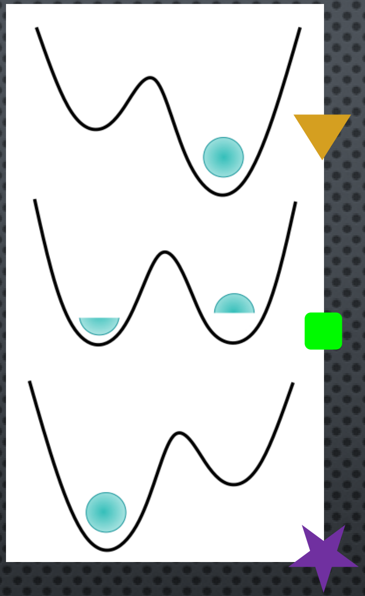

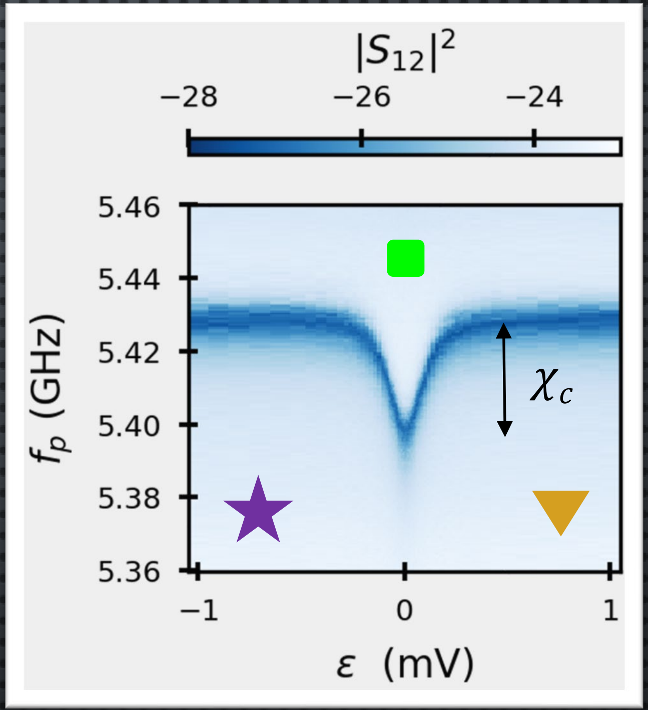

Cavity response to a probe field

$g_c/2\pi = 513$ MHz

$t_c/h = 9.6$ GHz

SPIN TRANSITION IN DQD WITH SOC

$B \neq 0$

No SOC

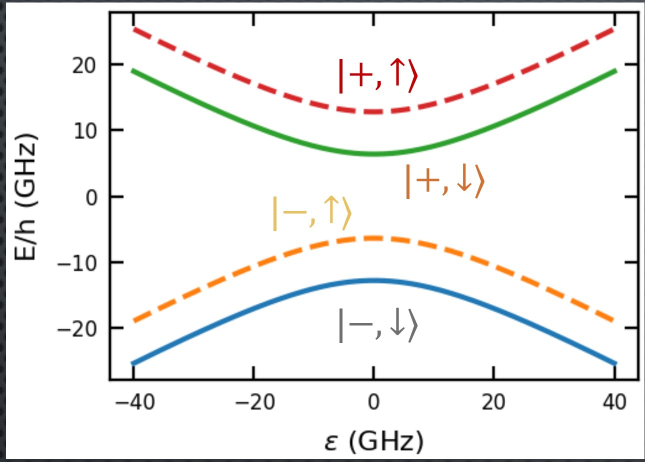

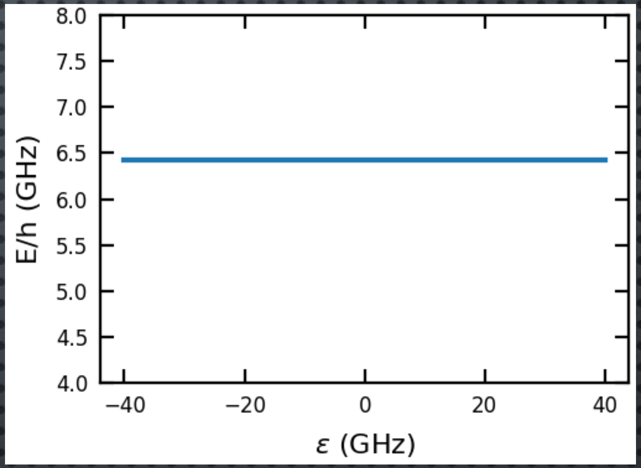

With SOC

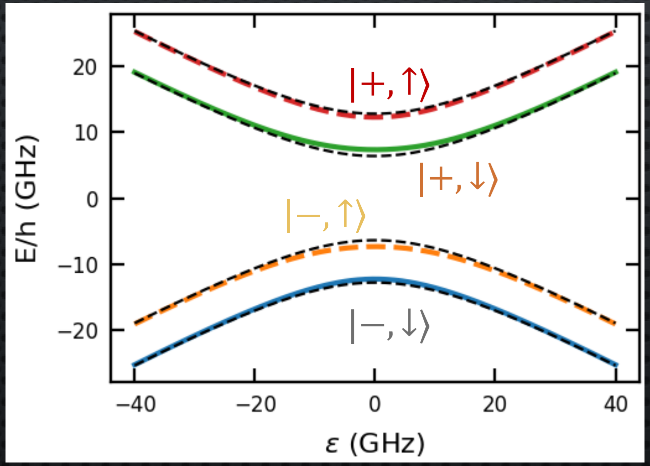

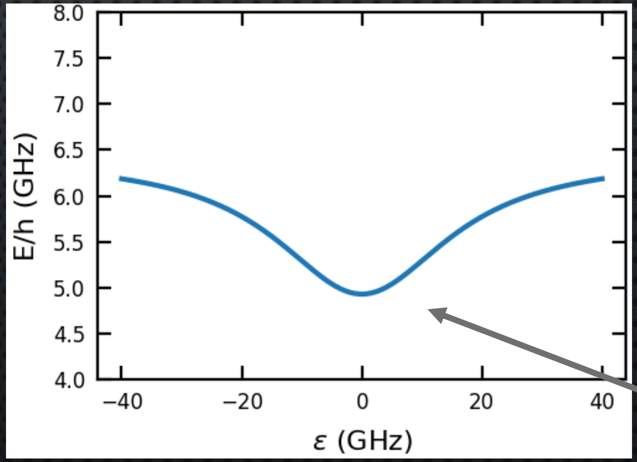

Sweet spot with respect
to charge noise

$$|-,\uparrow\rangle \longrightarrow \alpha|-,\uparrow\rangle + \beta|+,\downarrow\rangle$$

STRONG SPIN-PHOTON COUPLING

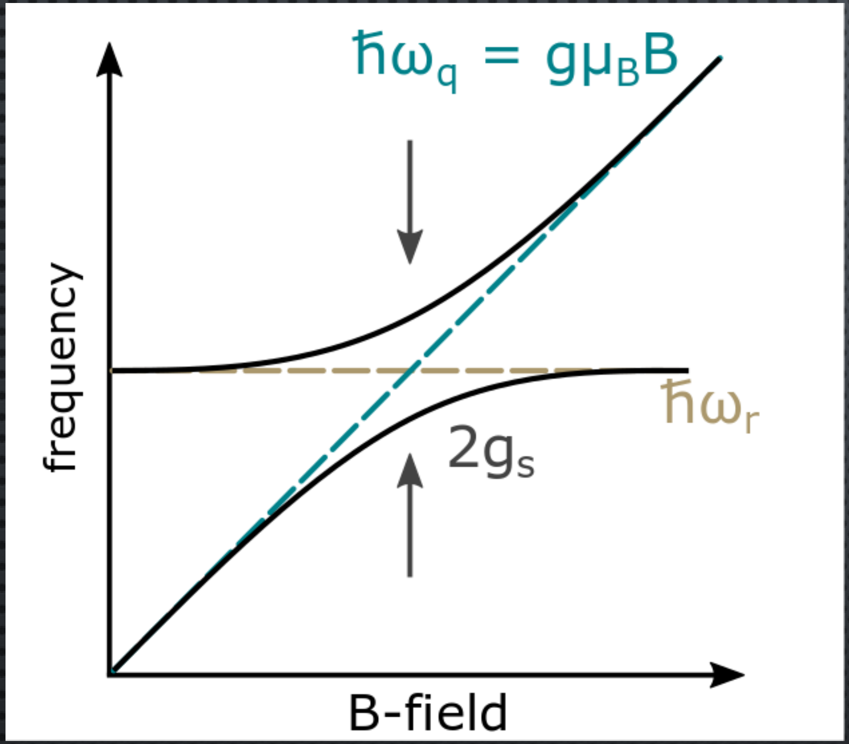

Vacuum Rabi mode splitting
→ signature of strong coupling

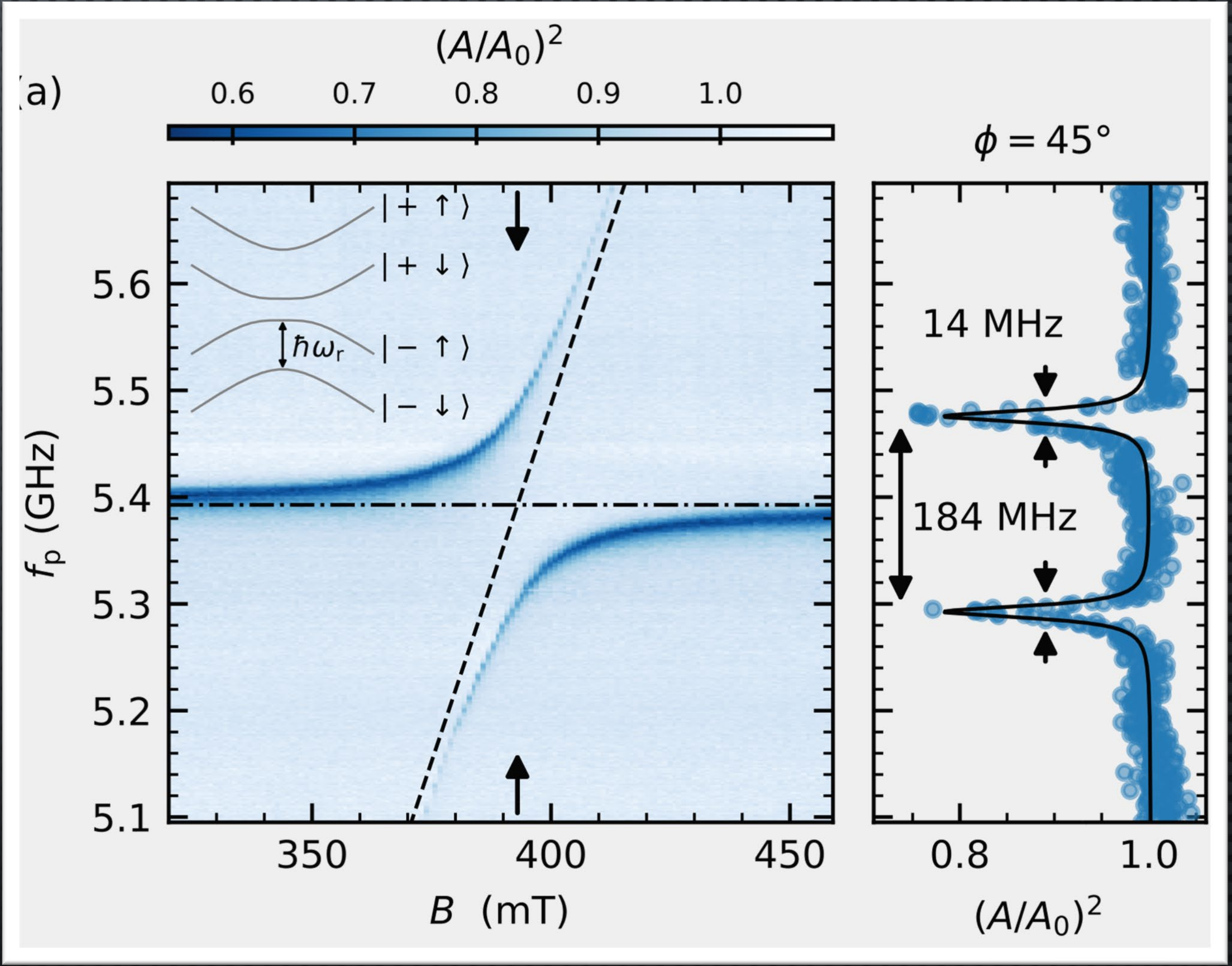

Strong spin-photon coupling with $2g_s/2\pi = 184$ MHz $\gg$ 13 MHz

STRONG SPIN-PHOTON COUPLING: ANGULAR DEPENDENCE

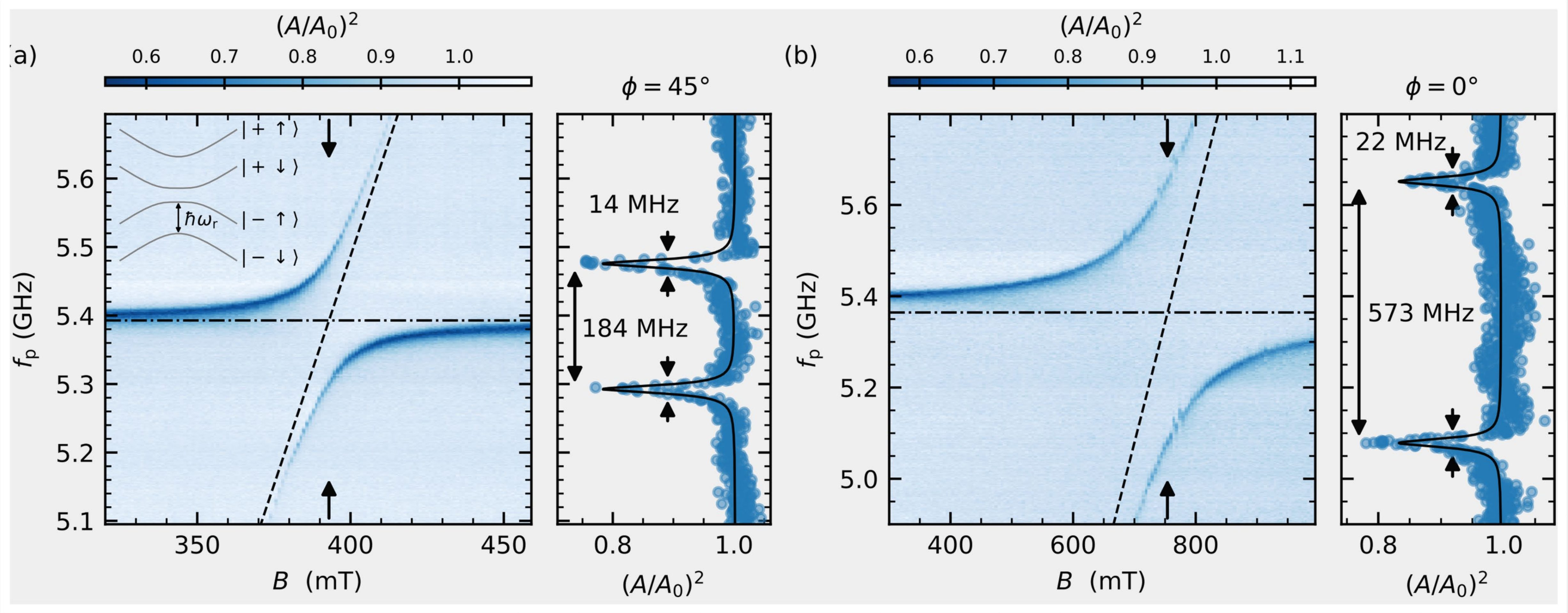

→ g_s heavily depends on the magnetic field orientation

ANGULAR DEPENDENCE

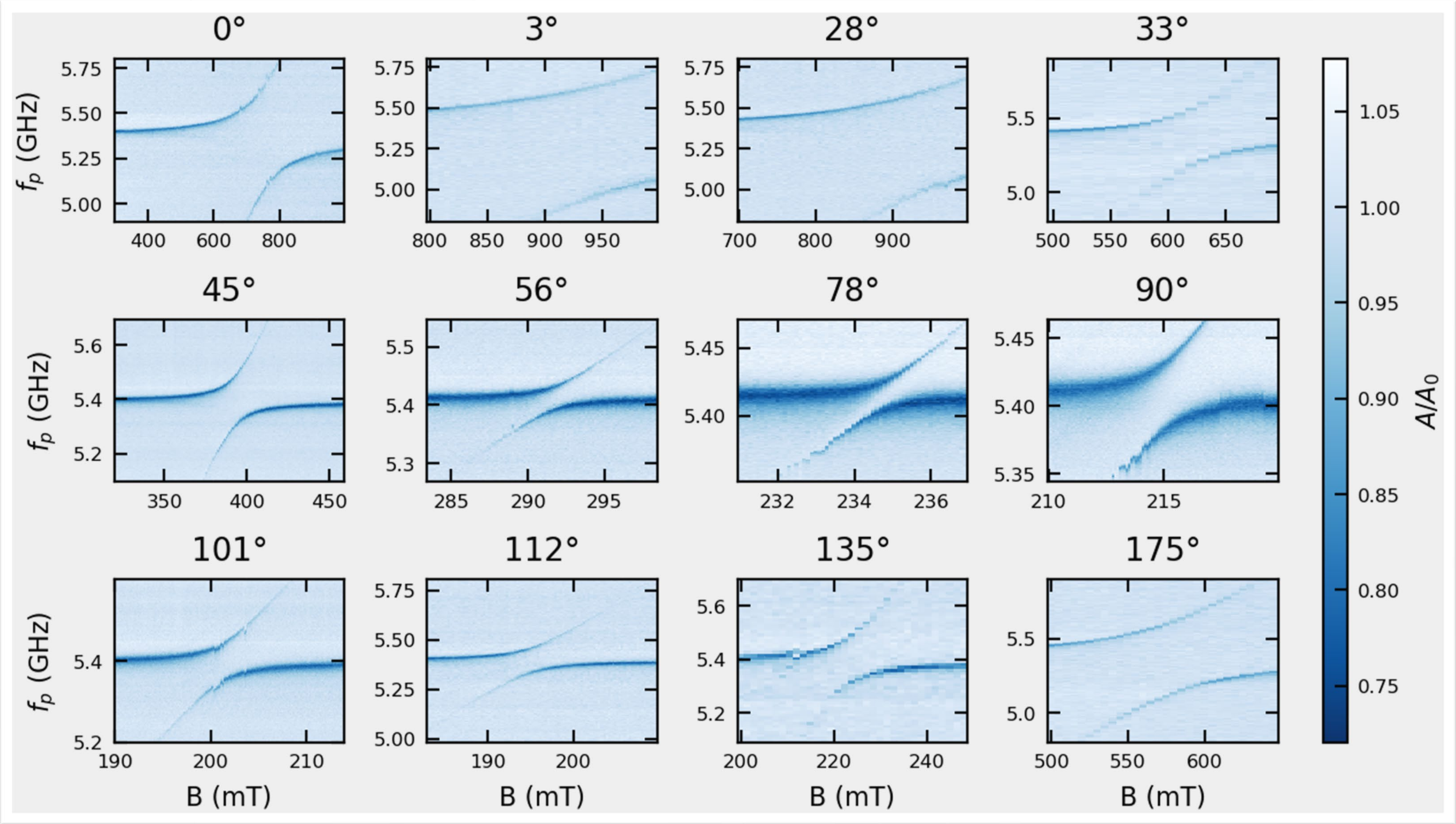

INTERPLAY BETWEEN ZEEMAN AND SO FIELD

$$H_{\mathrm{so}} = \frac{\hbar^2}{m_{||}\ell_{\mathrm{so}}} k_x B_{\mathrm{so}} \cdot \boldsymbol{\sigma}$$

B_{so} is the spin-orbit unit vector over which the spin precesses as it moves in x

ℓ_{so} is the length over which there is a spin flip

$$\mathrm{g}(\phi) \cdot \boldsymbol{B}$$

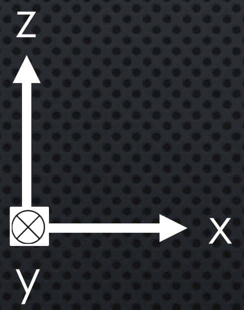

B_{so}

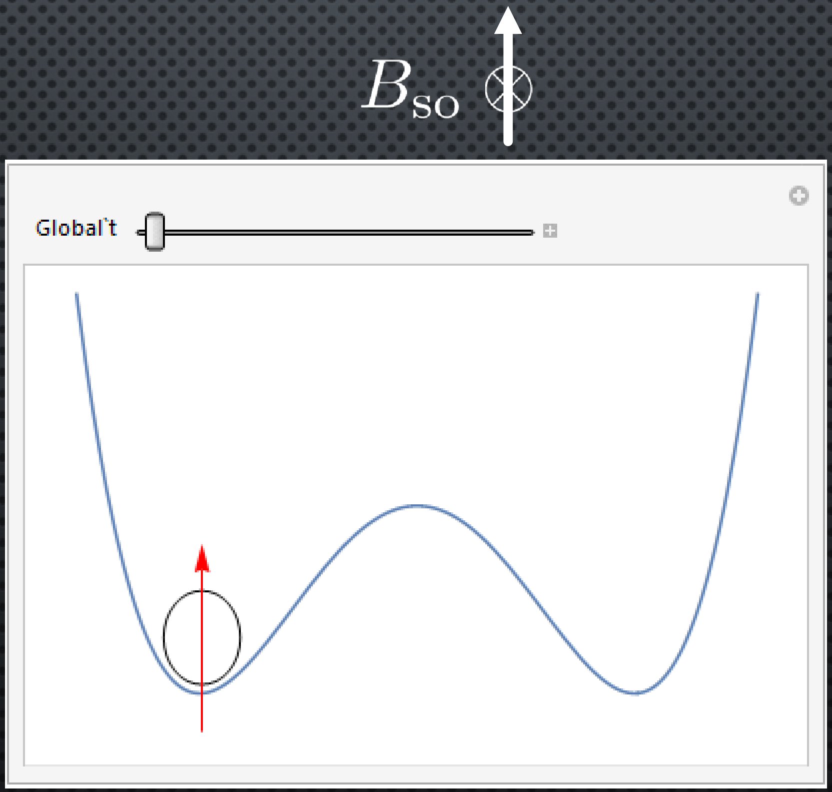

Tunneling flips the spin

Tunneling preserves the spin

In our case:

$$\ell_{so} \approx d$$

$$B_{so} \approx \hat{y}$$

STRONG SPIN-PHOTON COUPLING: ANGULAR DEPENDENCE

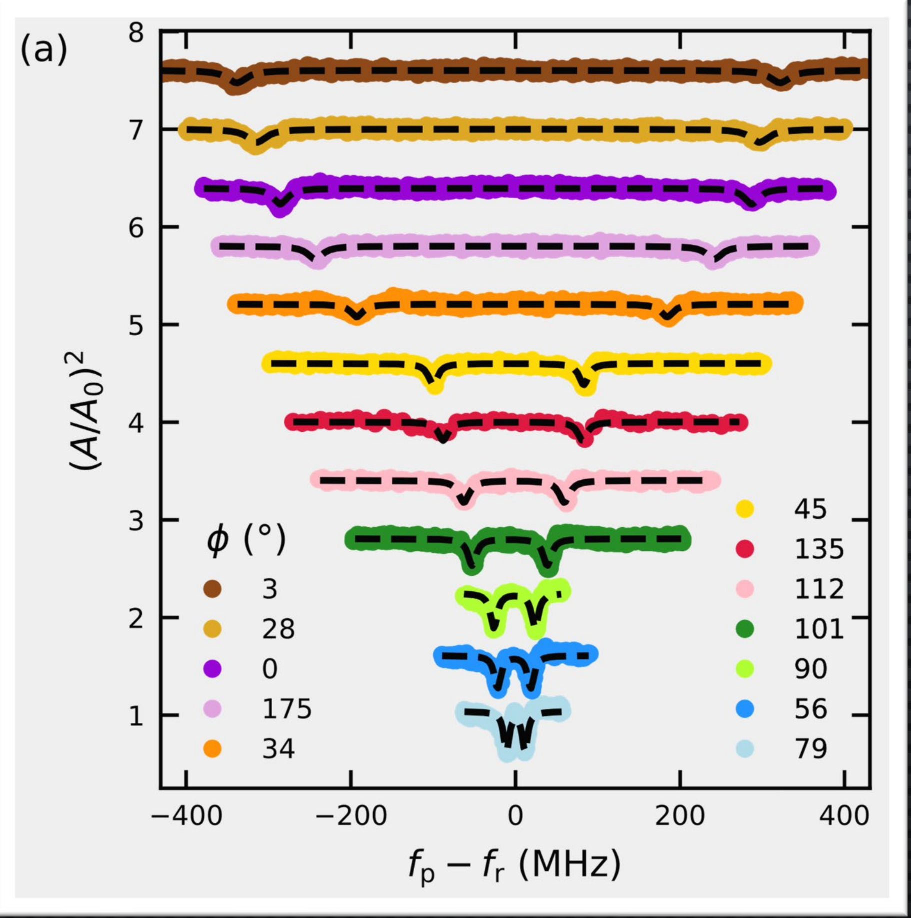

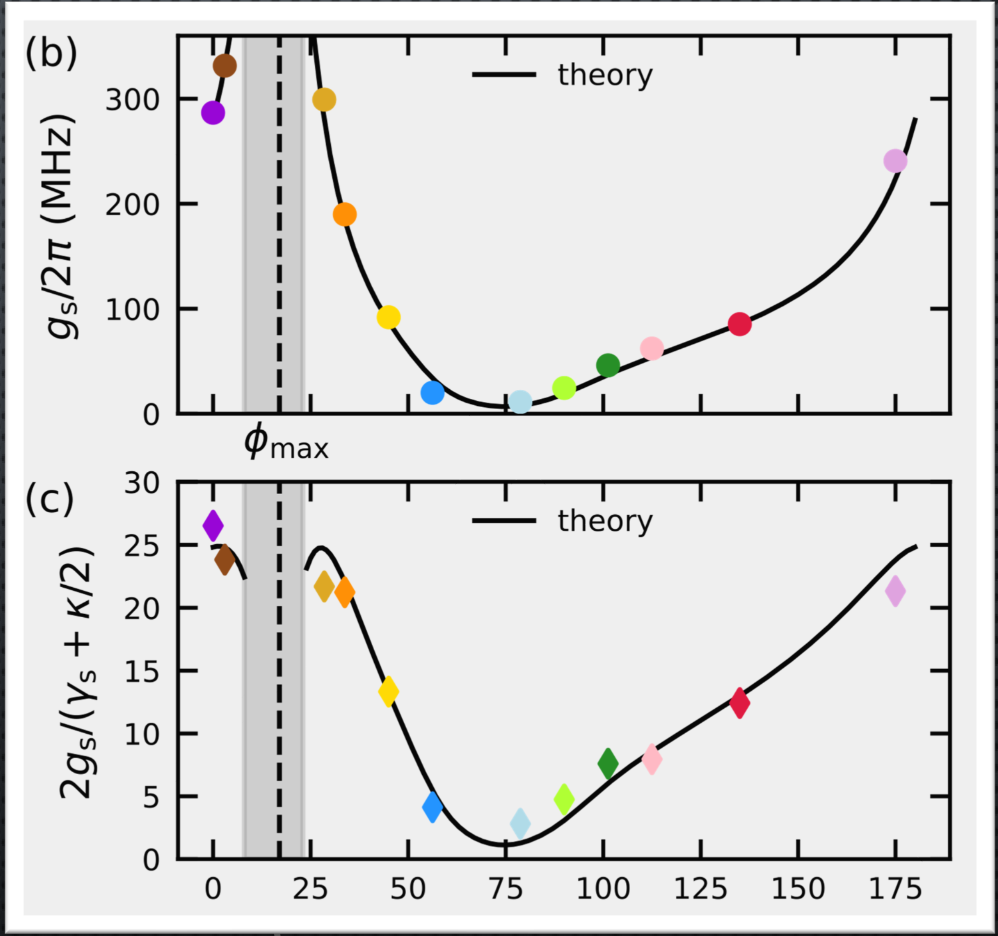

Max cooperativity

$$C = \frac{4g_s^2}{\gamma\kappa} = 1600$$

ϕ_{max} maximizes spin-photon coupling

$$g_s \propto g_c |(\hat{g} \cdot \vec{B}) \times \vec{B}_{so}|$$

SINGLE-DOT LIMIT

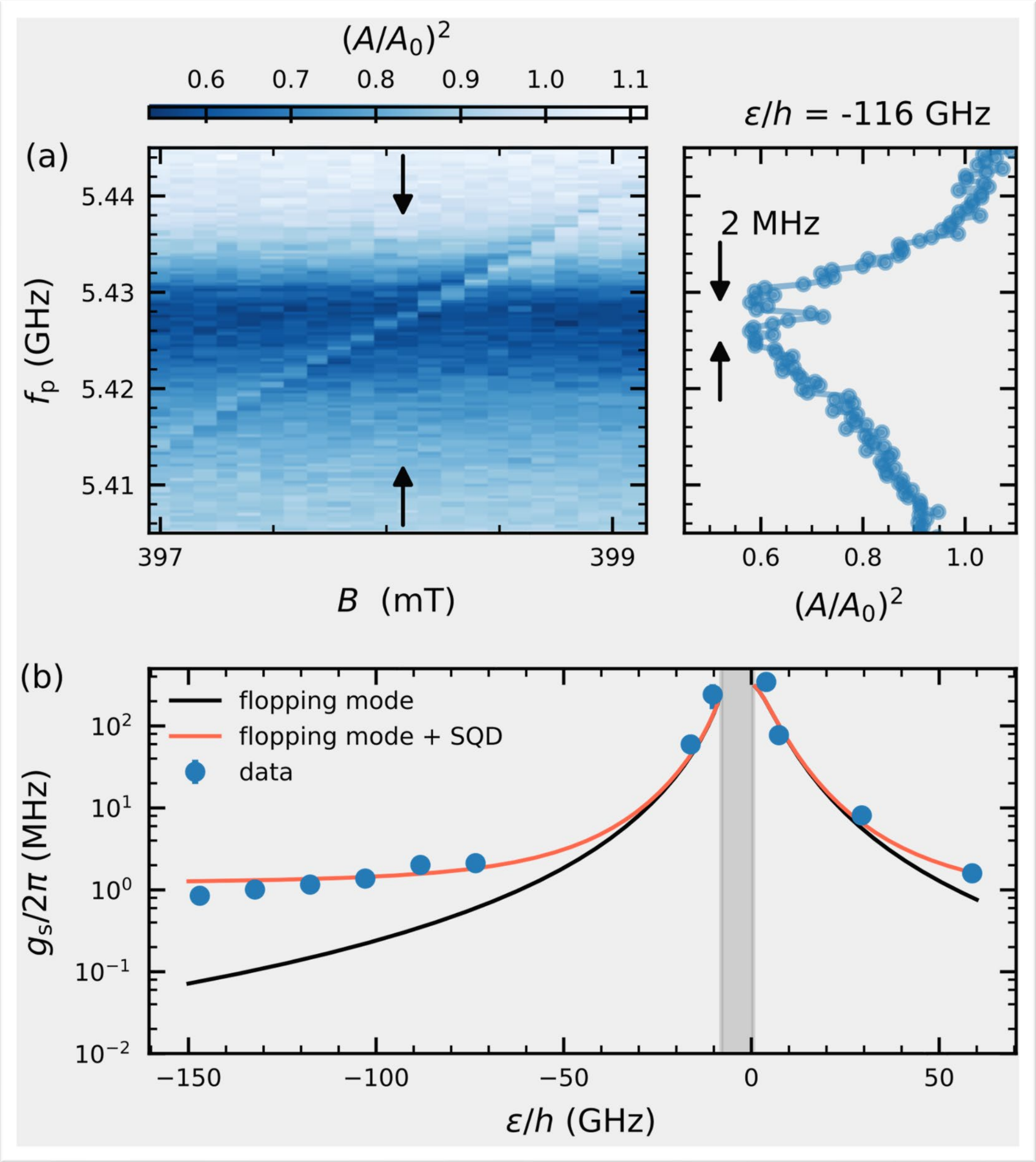

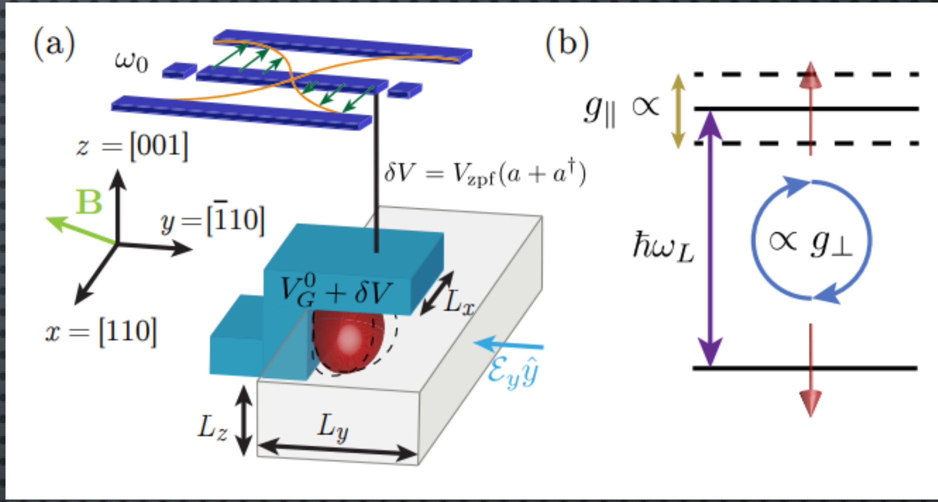

Michal et al. arXiv:2204.00404

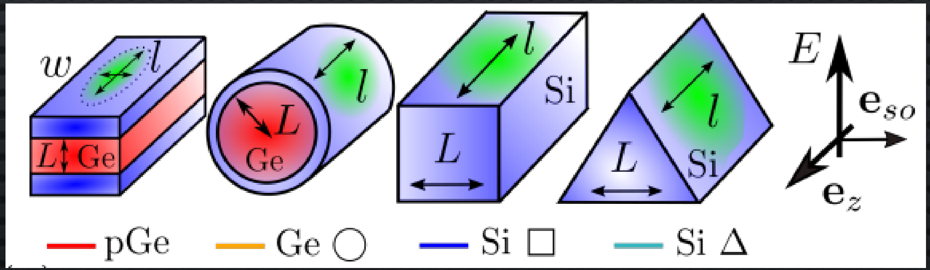

Bosco et al. arXiv:2203.17163

TAKE HOME MESSAGE

- Si-MOS hole spins embedded in a high-impedance cavity

- Bordering ultra-strong charge-photon coupling with $g_c = 513\ MHz$

- Unprecedented spin-photon coupling $g_s = 330$ MHz

- Extremely strong light-matter interaction, cooperativity of ~1600

- First demonstration of sizeable coupling in single dot limit $g_s \simeq$ 2 MHz

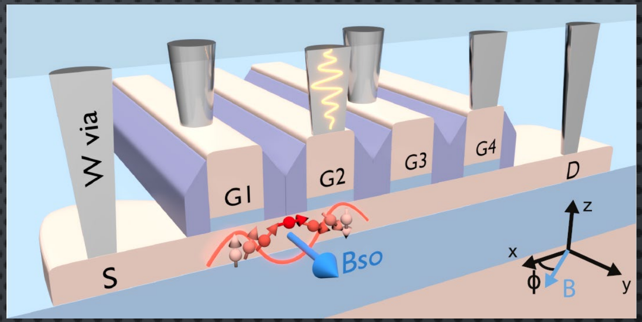

CONCLUSIONS

Holes are interesting creatures with cool physics still being unveiled

New mechanisms for manipulation: inhomogeneous electric fields: arXiv:2209.10231

Sweet spots with large coherence times: Nature Nanotechnology 17, 1072–1077 (2022)

Natural spin-photon coupling: arXiv:2206.14082

Single dot spin-photon architectures are possible: arXiv:2204.00404

CHARACTERIZING THE CHARGE-PHOTON COUPLING

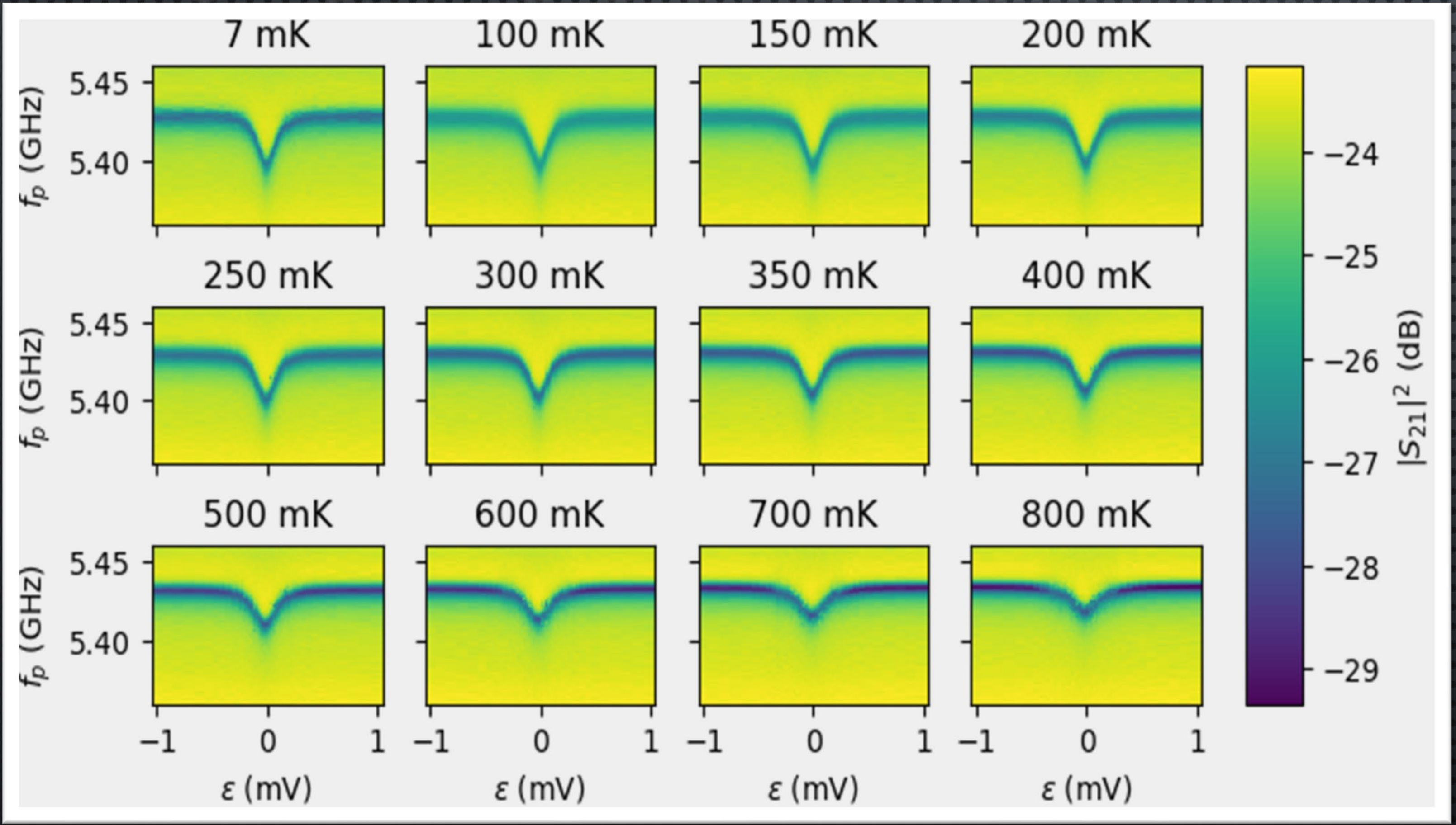

Dispersive shift at $\epsilon = 0$

$$\chi_c = g_c^2 \cdot (p_0 - p_1) \cdot \left(\frac{1}{\omega_q - \omega_r} + \frac{1}{\omega_q + \omega_r} \right)$$

$$p_1 = \frac{1}{1+e^{\hbar\omega_q/k_B T}}$$

$$p_0 = 1 - p_1$$

$g_c/2\pi = 513$ **MHz**

$t_c/h = 9.6$ **GHz**

ϵ VS B –MAPS: MEASUREMENT OF g_L, g_R AND SOI